Published in final edited form as:
Biochim Biophys Acta Mol Cell Biol Lipids. 2020 May 01; 1865(8): 158730. doi:10.1016/j.bbalip.2020.158730.

Lysosomal acid lipase is the major acid retinyl ester hydrolase in cultured human hepatic stellate cells but not essential for retinyl ester degradation

Carina Wagner[a], **Victoria Hois**[a], **Laura Pajed**[a], **Lisa-Maria Pusch**[a], **Heimo Wolinski**[a], **Michael Trauner**[b], **Robert Zimmermann**[a,c], **Ulrike Taschler**[a,*], **Achim Lass**[a,c,*]

[a]Institute of Molecular Biosciences, NAWI Graz, University of Graz, Heinrichstraße 31/II, A-8010 Graz, Austria

[b]Hans Popper Laboratory of Molecular Hepatology, Division of Gastroenterology and Hepatology, Department of Medicine III, Medical University of Vienna, Waehringer Guertel 18-20, A-1090 Vienna, Austria

[c]BioTechMed-Graz, Graz, Austria

Abstract

Vitamin A is stored as retinyl esters (REs) in lipid droplets of hepatic stellate cells (HSCs). To date, two different pathways are known to facilitate the breakdown of REs: (i) Hydrolysis of REs by neutral lipases, and (ii) whole lipid droplet degradation in autolysosomes by acid hydrolysis.

In this study, we evaluated the contribution of neutral and acid RE hydrolases to the breakdown of REs in human HSCs. (*R*)-Bromoenol lactone (R-BEL), inhibitor of adipose triglyceride lipase (ATGL) and patatin-like phospholipase domain-containing 3 (PNPLA3), the hormone-sensitive lipase (HSL) inhibitor 76-0079, as well as the serine-hydrolase inhibitor Orlistat reduced neutral RE hydrolase activity of LX-2 cell-lysates between 20 and 50%. Interestingly, in pulse-chase experiments, R-BEL, 76-0079, as well as Orlistat exerted little to no effect on cellular RE breakdown of LX-2 cells as well as primary human HSCs. In contrast, Lalistat2, a specific lysosomal acid lipase (LAL) inhibitor, virtually blunted acid *in vitro* RE hydrolase activity of LX-2 cells. Accordingly, HSCs isolated from LAL-deficient mice showed RE accumulation and were virtually devoid of acidic RE hydrolase activity. In pulse-chase experiments however, LAL-

*Corresponding authors at: Institute of Molecular Biosciences, University of Graz, Heinrichstraße 31/II, A-8010 Graz, Austria. ulrike.taschler@uni-graz.at (U. Taschler), achim.lass@uni-graz.at (A. Lass).

CRediT authorship contribution statement

Carina Wagner: Conceptualization, Writing - original draft, Writing - review & editing, Investigation, Methodology. **Victoria Hois**: Writing - review & editing, Investigation. **Laura Pajed**: Investigation, Writing - review & editing, Funding acquisition. **Lisa-Maria Pusch**: Investigation, Writing - review & editing, Methodology. **Heimo Wolinski**: Investigation, Data curation, Formal analysis, Methodology, Writing - review & editing. **Michael Trauner**: Data curation, Formal analysis, Resources, Writing - review & editing, Funding acquisition. **Robert Zimmermann**: Formal analysis, Resources, Writing - review & editing, Funding acquisition. **Ulrike Taschler**: Conceptualization, Investigation, Writing - review & editing, Validation, Supervision, Funding acquisition. **Achim Lass**: Conceptualization, Investigation, Writing - original draft, Writing - review & editing, Validation, Supervision, Project administration, Resources, Funding acquisition.

Declaration of competing interest

The authors declare that they have no known competing financial interests or personal relationships that could have appeared to influence the work reported in this paper.

Europe PMC Funders Author Manuscripts

deficient HSCs, similar to LX-2 cells and primary human HSCs, were not defective in degrading REs.

In summary, results demonstrate that ATGL, PNPLA3, and HSL cfontribute to neutral RE hydrolysis of human HSCs. LAL is the major acid RE hydrolase in HSCs. Yet, LAL is not limiting for RE degradation under serum-starvation. Together, results suggest that RE breakdown of HSCs is facilitated by (a) so far unknown, non-Orlistat inhibitable RE-hydrolase(s).

Keywords

Hepatic stellate cell; Retinol; Retinyl ester; Vitamin A; Lipase; Liver

1 Introduction

Hepatic stellate cells (HSCs) are specialized liver cells known to contain large amounts of retinyl esters (REs) [1]. These REs are stored in multi-locular cytosolic lipid droplets [2]. In times of insufficient dietary vitamin A supply, REs of HSCs are mobilized to maintain body's vitamin A requirements [3,4]. Under pathological conditions, the loss of hepatic REs is a hallmark for the progression of liver injury [5] and is associated with the activation of HSCs and their transformation into myofibroblast-like cells [6].

The degradation of REs requires the action of lipases. To date, two pathways have been shown to be involved in the breakdown of REs in HSCs: (i) One pathway is the degradation of REs of cytosolic lipid droplets by neutral RE hydrolases. (ii) The second pathway involves the engulfment of cytosolic lipid droplets, the storage site of REs, by autophagosomes and fusion with lysosomes, thereby forming autolysosomes [7]. Subsequently, engulfed lipid droplets are degraded in autolysosomes, a process termed lipophagy [8]. The enzyme responsible for acidic hydrolysis of lipids in autolysosomes is thought to be lysosomal acid lipase (LAL, annotated as lipase A). Consistent with a prominent role of LAL in acidic lipid hydrolysis, LAL-deficient mice are characterized by increased hepatic cholesteryl ester and triglyceride (TG) content [9]. However, LAL-deficient mice show decreased hepatic RE levels, arguing against a limiting role in hepatic RE breakdown [10].

Three neutral lipid hydrolases have been reported to hydrolyze REs at cytosolic lipid droplets: Adipose triglyceride lipase (ATGL, annotated as patatin-like phospholipase domain-containing 2, PNPLA2), hormone-sensitive lipase (HSL, annotated as lipase E), and adiponutrin (annotated as patatin-like phospholipase domain-containing 3, PNPLA3) [11–13]. The role of ATGL in RE degradation of murine HSCs has been studied in detail [13], and it has been demonstrated that ATGL does not play a rate-limiting role in this process. The expression level of HSL in HSCs is very low [13–15], implying that HSL does not play a pivotal role in this cell type. Accordingly, both ATGL and HSL knock-out (ko) mice have unchanged plasma retinol (ROH) levels and do not accumulate REs in the liver [13]. In liver, PNPLA3 is expressed not only in hepatocytes but also in HSCs and its expression is induced by carbohydrate feeding or insulin as well as during HSC activation [11,16–18]. In humans, the genetic variant I148M of PNPLA3 is the strongest predictor for increased risk of non-

Europe PMC Funders Author Manuscripts

alcoholic fatty liver disease and its progression to advanced fibrosis [19]. This I148M PNPLA3 variant exhibits reduced *in vitro* hydrolase activity against retinyl palmitate (RP), and human subjects carrying this I148M variant are associated with increased hepatic RP storage [11,20]. In contrast to human PNPLA3, the murine homologue does not exhibit detectable hydrolytic activity against REs [13]. Accordingly, PNPLA3-ko mice have not been reported to show changes in plasma ROH or hepatic RE levels.

In this study, we investigated the relative contribution of neutral and acid RE hydrolases in RE breakdown of human HSCs. We employed the human HSC cell-line LX-2 which is homozygous for the PNPLA3 I148M variant [18,21]. In addition, we also used human primary HSCs with wild-type (WT) PNPLA3 alleles (I148). Pharmacological inhibition of ATGL, PNPLA3, and HSL in RE hydrolase activity assays and pulse-chase experiments demonstrated a minor role of these lipases in neutral RE hydrolysis of human HSCs. In contrast, pharmacological inhibition of LAL virtually blunted acid RE hydrolase activity of human HSCs. However, in pulse-chase experiments, the pharmacological inhibition of LAL in human HSCs as well as genetical ablation of LAL expression in primary murine HSCs, isolated from LAL-ko mice, did not impair cellular RE breakdown. Together, these results indicate that LAL is the major acid RE hydrolase but that neither so far known neutral RE hydrolases nor LAL are limiting for RE degradation in HSCs.

2 Materials and methods

2.1 Materials

Essentially fatty acid (FA)-free bovine serum albumin (BSA), ROH, RP, retinyl acetate, triolein, L-α-phosphatidylinositol, 1,2-dioleoyl-snglycero-3-phosphocholine, and Orlistat were purchased from Sigma Aldrich (St. Louis, MO). Atglistatin®, Lalistat2, and the HSL inhibitor NNC 0076-0000-0079 (76-0079) were kind gifts from Dr. Rolf Breinbauer (Institute of Organic Chemistry, University of Technology, Graz, Austria), Dr. Paul Helquist (Department of Chemistry and Biochemistry, University of Notre Dame, Notre Dame, IN), and Dr. Christian Fledelius (Novo Nordisk A/S, Novo Nordisk Park, DK-2706 Måløv, Denmark), respectively. (*R*)-Bromoenol lactone (R-BEL) was purchased from Cayman Chemicals (Ann Arbor, MI). The human HSC line LX-2 was provided by Thierry Claudel, PhD (Hans Popper Laboratory of Molecular Hepatology, Division of Gastroenterology and Hepatology, Department of Medicine III, Medical University of Vienna, Vienna, Austria) with the kind approval of Dr. Scott L. Friedman (Icahn School of Medicine at Mount Sinai, New York, USA).

2.2 Methods

2.2.1 Cultivation of the human HSC cell-line LX-2—LX-2 cells were cultured in Dulbecco's Modified Eagle Medium (DMEM, 4.5 g/l glucose, Gibco®; Invitrogen GmbH, Lofer, Germany) supplemented with 1% fetal calf serum (FCS) and antibiotics at 37 °C under humidified atmosphere and 7% CO_2.

2.2.2 Husbandry of mice globally lacking LAL—Mice globally lacking LAL were generated as described previously [22] by consecutive breeding of Lipa$^{tm1a(EUCOMM)Hmgu}$

mice, carrying a FRT-flanked lacZ- reporter/neomycin selection cassette and a floxed exon 4 *Lipa* allele (targeted mutation 1a LAL^{tm1a}), with flippase and Cre recombinase expressing mice, which led to the excision of the reporter/selection cassette and of the exon 4 of the *Lipa* gene, respectively. Heterozygous LAL-deleter mice, lacking the exon 4 of the *Lipa* gene, were bred to receive homozygous LAL-deleter mice and WT controls. Mice globally lacking HSL (HSL-ko) were generated by targeted homologous recombination as described previously [23]. Mice were housed on a regular dark light cycle (14 h light, 10 h dark) at 22 ± 1 °C in a specific pathogen free environment and kept *ad libitum* on a standard laboratory chow diet (R/M-H Extrudate, V1126-037, Ssniff Spezialdiaeten GmbH, Soest, Germany). All animal experiments were approved by the Austrian Federal Ministry for Science, Research, and Economy (protocol number GZ: 39/9-4/75 ex 2017/18) and conducted in compliance with the council of Europe Convention (ETS 123).

2.2.3 Isolation of primary HSCs by collagenase perfusion and cultivation by selective detachment—Primary human HSCs were isolated from liver resections for metastasis of colon-rectal cancer, approved by the Ethic Committees of Medical University of Vienna (EK Nr: 2032/2013) as described [24]. HSCs were cultured in DMEM (4.5 g/l glucose; Gibco, Invitrogen) containing 10% FCS (Sigma Aldrich) and 100 μg/ml primocin. For experiments, primary human HSCs between passage 3 and 6 were used.

Primary HSCs of LAL-ko or HSL-ko mice and WT littermates (male/female, 2 months of age) were isolated as described previously by Blomhoff et al. [25] with some modifications. Briefly, mice were anesthetized and the abdomen was surgically opened. The liver was perfused *via* the portal vein with Krebs-Henseleit buffer (without Ca^{2+} and SO_4^{2-}) for 5 min, followed by a perfusion with Krebs-Henseleit buffer containing 0.2 mg/ml collagenase type II (Worthington Bio-chemical Corporation, Lakewood, NJ), 2% BSA, and 0.1 mM $CaCl_2$ for 10 min. Afterwards, the liver was excised, disrupted, and the cell suspension was passed through a gauze, followed by filtration through a 70 μm cell strainer. Hepatocytes were separated from non-parenchymal cells by centrifugation at 50 ×*g* for 3 min at 4 °C. Supernatant containing the non-parenchymal cell fraction was centrifuged at 900 ×*g* for 5 min at 4 °C. Pelleted non-parenchymal cells were suspended in DMEM (4.5 g/l glucose; Gibco, Invitrogen) containing 10% FCS (Sigma Aldrich) and 100 μg/ml primocin. Non-parenchymal cells were plated and cultivated at 37 °C in humidified air at 80% saturation and 5% CO_2. Non-cultivated primary HSCs were obtained by using OptiPrep™ self-forming density gradient solutions (Axis-Shield PoC AS, Rodeløkka, Norway) according to manufacturer's instructions. Non-parenchymal cell suspension was adjusted to a density of 24% iodixanol, overlaid with 11.5%, 8.4%, and 0% iodixanol in Krebs-Henseleit buffer containing 1.25 mM $CaCl_2$ and 1.2 mM Na_2SO_4. After centrifugation at 1400 ×*g* for 20 min at 4 °C, stellate cells were isolated at 8.4/0% iodixanol interphase [26].

Cultures of primary HSCs were obtained by selective detachment for 12–14 days. After 2 days in culture, cells were trypsinized and seeded again. This resulted in the removal of non-stellate cells from the culture. After 10 days of culture, > 90% of cells stained positive for alpha-smooth muscle actin (α-SMA) [13].

2.2.4 Lipid loading of HSCs and pulse-chase experiments—To promote lipid droplet formation, LX-2 cells or primary HSCs were incubated for 16–20 h in DMEM (4.5 g/l glucose) supplemented with 10% FCS, 40 μM or 20 μM ROH (40 mM stock solution in ethanol), and 300 μM or 100 μM oleic acid (4 mM stock solution in PBS, complexed to essentially FA-free BSA in a ratio of 3:1, M/M), respectively. Then, media was replaced with serum-free DMEM (1 g/l glucose) supplemented with 2% FA-free BSA (serum-starvation) and cells were incubated for 8 h. In some cases, media contained pharmacological inhibitors such as Lalistat2, Orlistat, R-BEL, and HSL inhibitor 76-0079 at a concentration of 20 μM.

2.2.5 Isolation of total RNA and analysis of gene expression by quantitative real-time PCR (qPCR)—HSC LX-2 cells were lysed by addition of 1 ml TRIzol™ and incubation at room temperature for 5 min. Phase separation was performed by addition of 100 μl 1-bromo-3-chloropropane and centrifugation at 12,000 ×*g* and 4 °C for 15 min. Supernatant was transferred and total RNA was precipitated by addition of 500 μl 2-propanol and centrifugation at 12,000 ×*g* and 4 °C for 10 min. RNA was washed twice with 70% ethanol and centrifugation at 7500 ×*g* and 4 °C for 5 min. DNA digestion was performed with DNase I and RNA was reverse-transcribed into cDNA using LunaScriptTM RT SuperMix kit (New England Biolabs). qPCR was performed as described previously [27]. The following primers were used: PNPLA2_forward: 5′-GTG TCA GAC GGC GAG AAT G -3′; PNPLA2_reverse: 5′- TGG AGG GAG GGA GGG ATG -3′; LIPE_forward: 5′- CTG CAT AAG GGA TGC TTC TAT GG -3′; LIPE_reverse: 5′- GCC TGT CTC GTT GCG TTT G -3′; PNPLA3_forward: 5′- GGC ATC TCT CTT ACC AGA GTG T -3′; PNPLA3_reverse: 5′- GGC ATC CAC GAC TTC GTC TTT -3′; ABHD5_-forward: 5′-ACA GAC CTG TCT ATG CTT TTG AC -3′; ABHD5_reverse: 5′- AGG GCA CAT CTC CAC TCT TCA -3′; 36B4_forward: 5′- GCT TCA TTG TGG GAG CAG ACA -3′; 36B4_reverse: 5`- CAT GGT GTT CTT GCC CAT CAG-3′. Target gene expression was calculated by the ΔΔCT method. Expression of ribosomal housekeeping gene *36b4* was used for normalization.

2.2.6 Microscopy—Primary HSCs were cultivated in chamber slides. To promote lipid droplet formation, cells were incubated with ROH and oleic acid as described above. Lysosomes were stained with LysoTracker Red DND-99 (Invitrogen™, ThermoFisher Scientific, Waltham, MA) for 45 min at 37 °C. After staining, cells were washed twice with PBS. Microscopy was performed on a Leica SP5 confocal microscope (Leica Microsystems Inc., Germany) using a 63×, NA 1.4 HCX PL APO oil immersion objective. LysoTracker was excited at 561 nm and detected in the range between 580 and 620 nm.

Coherent anti-Stokes Raman scattering (CARS) microscopy of primary HSCs was performed using a commercial setup consisting of a two-photon picosecond laser source (picoEmerald; APE, Berlin, Germany), integrated into the confocal microscope. To achieve the CARS effect and to detect CH_2 symmetric stretching vibrations of neutral lipids, cells were simultaneously illuminated at 816.7 nm and at 1064 nm using the picosecond laser source. The CARS signal was detected using a non-descanned detector in (forward-) CARS mode and a 465/170 nm bandpass filter. To discriminate between CARS signal of neutral

lipids and of observed additional two-photon excited autofluorescence of cellular structures, samples were simultaneously excited at 816.7 and 1064 nm (CARS and autofluorescence signal) as well as at 816.7 nm without the 1064 nm line (only autofluorescence signal).

2.2.7 Preparation of cell lysates and determination of protein content—Cell lysates were prepared from a cell suspension in solution A (0.25 M sucrose, 1 mM EDTA, 1 mM DTT, 20 μg/ml leupeptin, 2 μg/ml antipain, and 1 μg/ml pepstatin, pH 7.0) by sonication (2 × 10 s, amplitude 15%; Sonoplus ultrasonic homogenizer HD3100, Bandeline electronic GmbH & Co. KG, Berlin, Germany). Nuclei and unbroken cells were removed by centrifugation at 1000 ×*g* for 10 min at 4 °C and lysates were stored at −20 °C until further use. Protein concentrations were determined by Bio-Rad protein assay according to manufacturer's instructions using BSA as standard (Bio-Rad, Hercules, CA).

2.2.8 Extraction of neutral lipids for HPLC-fluorescence detection (FD) analyses and thin-layer chromatography—Cells were washed twice with PBS. Neutral lipids were extracted twice with 1 ml *n*-hexane:2-propanol (3:2; v/v) for 10 min under constant shaking at room temperature. Organic phases were combined and dried in a speed-vac (Labconco, Kansas City, MO). For retinoid analysis, dried lipids were dissolved in methanol:toluene (1:1, v/v) and applied to HPLC-FD analysis (see below). For TG analysis, dried lipids were dissolved in chloroform and applied on a silica gel coated aluminum plate (Merck KGaA, Darmstadt, Germany). Thin-layer chromatography plates were developed in a mixture of *n*-hexane:diethylether:glacial acetic acid (70:29:1, v/v/v). Lipids were stained with 10% phosphoric acid containing 10% copper (II) sulfate and heating at 120 °C for 15–30 min.

2.2.9 Oil Red O staining of neutral lipids—LX-2 cells were seeded in 12-well plates and cultivated under standard culture conditions. In some cases, cells were loaded with ROH and oleic acid as described above. Afterwards, cells were washed twice with PBS and fixed with 4% para-formaldehyde for 15 min. Then, cells were washed twice with H_2O and once with 60% 2-propanol. Air-dried cells were stained with Oil Red O staining solution for 45 min. Cells were washed twice with H_2O. Microscopic evaluation was performed using an inverted light microscopy (amplification 10×; Nikon eclipse TE300).

2.2.10 Quantification of retinoids by HPLC-FD—Lipid extracts, dissolved in methanol:toluene (1:1, v/v), were separated on a YMC-Pro C18 column (150 × 4.6 mm, S-5 μl, 12 nm, YMC Europe GmbH, Dinslaken, Germany) using a gradient solvent system (flow, 1 ml/min; gradient, 1–5 min 100% methanol, 5–14 min 60%/40% methanol/toluene, and 14–18 min 100% methanol). Fluorescence was detected at excitation 325 nm/emission 490 nm. The HPLC consisted of a Waters e2695 separation module, a column oven (at 25 °C), and a Waters 2475 fluorescence detector (Waters Corp., Milford, MA). Data were analyzed using Empower 3 chromatography data software (Waters Corp.).

2.2.11 Analysis of protein expression levels by immunoblotting—Proteins of cell lysates (10–40 μg protein) were dissolved in SDS sample buffer, separated by 10% or 12.5% SDS-PAGE, and transferred onto a PVDF membrane (Carl Roth GmbH, Karlsruhe, Germany). The membrane was blocked with 10% non-fat dry milk and probed with

following primary antibodies: anti-ATGL, anti-HSL, anti-lysosomal-associated membrane protein 1 (LAMP1), anti-ras-related protein 7 (RAB7), anti-autophagy related 7 (ATG7), anti-microtubule-associated protein 1B-light chain 3 (LC-3B), anti-sequestosome-1 (p62), and anti-glyceraldehyde 3-phosphate dehydrogenase (GAPDH) from Cell Signaling Technology (2138S/ATGL, 4107S/HSL, 3243/LAMP1, 2094S/RAB7, 8558S/ATG7, 2775S/LC-3B, 5114S/p62, and 2118S/GAPDH), anti-comparative gene identification-58 (CGI-58) from Abnova (H000051099-M01), anti-α-SMA from Thermo Scientific (PA5-22251), anti-PNPLA3 from Abcam (ab81874), and anti-adipose differentiation-related protein (ADRP) from Progen (GP40), respectively. For detection, membranes were incubated with horseradish peroxidase labeled secondary antibodies specific for respective primary antibody. Bands were visualized using the ECL plus Western blotting Detection Reagent (Fisher Scientific, Waltham, MA) and ChemiDoc Touch Imaging System (Bio-Rad, Hercules, CA).

2.2.12 Measurement of in vitro RE hydrolase activity—RE hydrolase activity assay was performed as described previously [10] with some modifications. Briefly, 100 μl cell lysates (50–100 μg protein) were incubated with 100 μl substrate for 1 h at 37 °C in a water bath under constant shaking. The substrate consisted of RP (300 μM), emulsified with phosphatidylcholine (PC, 300 μM) or a mixture of PC (225 μM) and phosphatidylinositol (PI, 75 μM) as indicated in the figure legends. For substrate preparations, lipids were dried under N_2 and emulsified in 100 mM sodium acetate buffer (pH 4.5) or 100 mM potassium phosphate buffer (pH 7.5) by sonication. Substrates of different pH were obtained by adding 100 mM sodium acetate buffer of the pH range of 4.0–6.5 or Bis-Tris propane buffer of the pH range 6.0–8.5 to the substrate preparation (emulsified in 50 mM potassium chloride buffer). Then, 4% FA-free BSA was added to the substrate and mixed by vortexing. Substrate blank incubation was performed with solution A. After incubation, 1 ml *n*-hexane and 200 μl ethanol, containing 1.14 μM retinyl acetate as internal standard, were added. Samples were vigorously vortexed and phase separation was obtained by centrifugation at 5000 ×*g* at 4 °C for 10 min. Upper organic phase (800 μl) was collected and dried in a speed-vac. Samples were dissolved in 100 μl methanol:toluene (1:1, v/v) and analyzed by HPLC-FD.

2.2.13 Measurement of in vitro TG hydrolase activity—TG hydrolase activity assay was performed as described previously [28] with some modifications. In brief, 100 μl cell lysates (50–100 μg protein) were incubated with 100 μl substrate for 1 h at 37 °C. The substrate contained triolein (300 μM) and [^{3}H]-triolein (10 μCi/ml) and was emulsified with PC:PI (3:1, M/M; 45 μM). Lipids were dried under N2 and emulsified by sonication in 100 mM sodium acetate buffer (pH 4.5) or 100 mM potassium phosphate buffer (pH 7.5). Then, 5% FA-free BSA was added and mixed by vortexing. Reactions were terminated by addition of 3.25 ml methanol:chloroform:*n*-heptane (10:9:7, v/v/v) and 1 ml 0.1 M potassium carbonate (pH 10.5). Then, samples were vigorously vortexed and centrifuged at 2000 ×*g* for 10 min. The radioactivity in 500 μl of the upper phase was determined by liquid scintillation counting. Substrate blank incubation was performed with solution A.

2.2.14 Statistical analyses—Data are presented as mean + standard deviation (S.D.). Statistically significant differences were determined by Student's unpaired *t*-test (two-tailed). Group differences were considered statistically significant for $p < 0.05$ (*), $p < 0.01$ (**), and $p < 0.001$ (***).

3 Results

3.1 Neutral RE hydrolase activity of human HSC cell-line LX-2 is partially inhibited by Orlistat

To characterize RE hydrolase activity of the human HSC cell-line LX-2, we first measured pH-dependent hydrolysis of RP in *in vitro* activity assays using cell lysates. We observed a pH optimum of around 6.5–7, with a steep decline in RE hydrolase activity at pH values higher than 8 (Fig. 1A). Addition of the non-selective serine-hydrolase inhibitor Orlistat [29] reduced RE hydrolase activity over the entire pH range by ~50% (Fig. 1A). Orlistat is known to inhibit lipases such as ATGL and HSL [30], which are able to hydrolyze REs [12,13]. Thus, we analyzed mRNA and protein expression levels of known RE hydrolases by qPCR and Western blotting, respectively. Expression of *PNPLA2* (=ATGL), *α/β hydrolase domain-containing protein 5* (*ABHD5* = comparative gene identification-58, CGI-58), known to interact with ATGL and PNPLA3 [31,32], *lipase E* (*LIPE* = HSL), and *PNPLA3* was detectable by qPCR and Western blotting (Fig. 1B, C). Interestingly, mRNA expression of *PNPLA2* was highest and that of *ABHD5*, *LIPE*, and *PNPLA3* in the order of 50 to 90% lower than that of *PNPLA2* (Fig. 1B). Antibodies specific for ATGL, PNPLA3, CGI-58, HSL, and GAPDH (as loading control) showed bands at respective molecular weights, albeit intensities did not match that of the qPCR measurements (Fig. 1C). To dissect the contribution of ATGL, PNPLA3, and HSL to neutral RE hydrolase activity in lysates of LX-2 cells, we employed several enzyme inhibitors. Addition of R-BEL, a compound known to inhibit ATGL and PNPLA3 [33,34], and 76-0079, a specific inhibitor of HSL [35], decreased *in vitro* RE hydrolase activity of LX-2 cell lysates by 13 and 25%, respectively (Fig. 1D). Addition of the general serine-hydrolase inhibitor Orlistat [29] and the unspecific serine-protease inhibitor phenylmethylsulfonylfluoride (PMSF) [36] reduced RE hydrolase activities by 41 and 35%, respectively (Fig. 1D). Heat inactivation of lysates virtually blunted RE hydrolase activity of LX-2 cell lysates (Fig. 1D). Results of this inhibitor study indicate that ATGL, PNPLA3, and HSL contribute to neutral RE hydrolase activity of LX-2 cells together by around 40%. The remaining 60% of neutral RE hydrolase activity is insensitive to the applied serine-hydrolase inhibitors.

ATGL, PNPLA3, and HSL have been shown to be expressed in HSCs [11,13,37]. Furthermore, they exhibit TG hydrolase activity [38–41], while HSL is known to be rate-limiting for diglyceride hydrolysis [23]. Thus, as a proof of concept and to demonstrate that the small molecule inhibitors effectively inhibit hydrolases in our *in vitro* assay system, we performed TG hydrolase activity assays using again cell lysates of LX-2 cells and radiolabeled triolein as substrate. As expected, we observed that addition of R-BEL and Orlistat effectively reduced TG hydrolase activity (40% and down to n.d., respectively), while the HSL-specific inhibitor 76-0079 exerted virtually no effect. The combination of R-BEL and 76-0079 did not further reduce TG hydrolase activity, compared to R-BEL alone

(Suppl. Fig. 1A). Furthermore, addition of purified CGI-58 to the incubation mixture led to increased TG hydrolase activity (~2-fold) (Suppl. Fig. 1B). Since TG hydrolase activity of LX-2 lysates was stimulated by CGI-58 and inhibited by R-BEL, it is conclusive that ATGL and presumably also PNPLA3 contribute to TG hydrolysis in human HSCs.

3.2 ATGL, PNPLA3, and HSL are not limiting for the breakdown of REs in human HSCs

The observation that small molecule inhibitors, known to inhibit ATGL, PNPLA3, and HSL, inhibited *in vitro* RE hydrolase activity of LX-2 cell lysates, prompted us to study RE degradation in cell culture experiments. Under standard culture conditions, LX-2 cells contain only low amounts of REs. Thus, to promote RE synthesis and lipid droplet formation, we loaded cells with a combination of ROH and oleic acid. As expected, after ROH/oleic acid loading of cells, numerous lipid droplets were visible, as evident by round structures stainable by Oil Red O (Suppl. Fig. 2A). Consistent with increased Oil Red O staining of cells, lipid loaded LX-2 cells contained 370-fold increased RP content (Suppl. Fig. 2B). Furthermore, ROH/oleic acid loading of cells also induced TG accumulation, as evident from respective bands on the thinlayer chromatogram (Suppl. Fig. 2C).

Next, we performed pulse-chase experiments where we loaded LX-2 cells with ROH/oleic acid and then serum-starved cells in the absence or presence of various inhibitors. At all indicated time points, we measured cellular RP and TG contents as well as the amounts of ROH and non-esterified fatty acids (NEFAs) in the incubation media (for schematic representation of experiment see Fig. 2A). Under all culture conditions, protein expression of HSL, ATGL, and PNPLA3 were detectable, as assessed by Western blotting (Fig. 2B). While no apparent differences of HSL protein was observed between culture conditions, protein levels of ATGL increased upon lipid loading and remained high during serum-starvation (Fig. 2B). Interestingly, in accordance with previous reports [16], protein levels of PNPLA3 decreased upon serumstarvation (Fig. 2B). Lipid loading of cells strongly increased cellular RP and TG contents (compare “basal” *vs* “loaded” in Fig. 2C and E). After serum-starvation (chase period), cellular RP and TG contents of control incubation (DMSO) declined by 52 and 34%, respectively, indicative for the hydrolysis of these lipid esters. The addition of the inhibitors R-BEL or Orlistat during the chase period did not attenuate, while addition of 76-0079 slightly accelerated cellular RP breakdown (Fig. 2C). The presence of the HSL inhibitor 76-0079 moderately decreased ROH content in the incubation media, while other inhibitors had no effect (Fig. 2D). In contrast to cellular RP levels, LX-2 cells incubated in the presence of R-BEL showed 30% higher cellular TG levels, whereas 76-0079 and Orlistat had no effect (Fig. 2E). Furthermore, R-BEL and Orlistat, but not 76-0079 significantly reduced the amounts of NEFA in the incubation media (by 33 and 58%, respectively) (Fig. 2F).

Since LX-2 cells are known to be homozygous for the I148M PNPLA3 variant, which exhibits reduced RE hydrolase activity as compared to WT PNPLA3 [11], we also performed similar pulse-chase experiments with primary human HSCs. Similar as observed with LX-2 cell-line, also primary human HSCs accumulated RP upon lipid loading which was largely degraded after the serum-starvation period (Fig. 2G). The presence of the

inhibitor R-BEL reduced RE degradation by 25%, while the inhibitors 76-0079 and Orlistat had no effect (Fig. 2G).

Together, the observation that none of the inhibitors largely impaired cellular RE degradation of human HSCs during a serum-starvation period indicated that the hydrolases ATGL, PNPLA3, and HSL contribute to a minor extent to RE hydrolysis of human HSCs.

The role of ATGL in the hydrolysis of REs has been studied in murine primary ATGL-deficient HSCs [13]. Since we had access to primary murine HSL-ko HSCs, we investigated murine HSL in pulse-chase experiments. Western blotting of cell lysates of primary murine HSCs confirmed the knockout of HSL protein (Suppl. Fig. 3A). Loading of WT as well as of HSL-ko murine primary HSCs led to many-fold increased cellular RP levels, which altogether declined to a similar extend after the serum-starvation period (Suppl. Fig. 3B), confirming that also a genetic deletion of HSL does not attenuate RE loss of HSCs under serum starvation.

3.3 LAL accounts for the majority of acid RE hydrolase activity in human HSC cell-line LX-2

To characterize acid RE hydrolase activity of human HSC LX-2 cells, we first optimized the reaction conditions for acid RE hydrolase activity. Negatively charged phospholipids such as PI or bis (monoacylglycero)phosphate are known to stimulate acid hydrolytic activity of LAL [10,42]. Interestingly, rates of acid RE hydrolase activity in *in vitro* activity assays using lysates of LX-2 cells were ~3-fold higher when the substrate was emulsified with the addition of PI, in comparison to PC alone (Fig. 3A). Furthermore, addition of the LAL-specific inhibitor Lalistat2 [43] to the assay mixture decreased acid RE hydrolase activity of lysates from LX-2 cells by 97% (Fig. 3B). pH-dependent measurements of RE hydrolase activities of LX-2 cell lysates in the acidic range gave highest activities between pH 4 and 5 (Fig. 3C). Addition of Lalistat2 to the incubation mixture almost completely blunted RE hydrolase activities (by > 95%) in the pH range of 4 to 5 (Fig. 3C), suggesting that LAL is the major acid RE hydrolase in LX-2 cells.

3.4 LAL-specific inhibitor Lalistat2 partially inhibits the breakdown of REs of human HSCs

To examine the role of LAL in RE degradation in a cellular context, we performed pulse-chase experiments using Lalistat2 and the human HSC cell-line LX-2. After loading of LX-2 cells with ROH/oleic acid, cells were incubated in the absence or presence of Lalistat2 in the subsequent serum-starvation (chase) period. Then, the cellular RP and TG contents and the amounts of ROH and NEFA in the incubation media were determined (for schematic representation of experiment see Fig. 4A). After the serum-starvation/chase period, the cellular RP content of control cells (DMSO) declined by 38%. Lalistat2-treated cells contained 40% more cellular RP than control cells (Fig. 4B). The amount of ROH in the incubation media of DMSO *vs* Lalistat2-treated cells after the serum starvation period was virtually unchanged (Fig. 4C). In line with higher cellular RP levels upon Lalistat2 treatment, also cellular TG levels were 30% higher in Lalistat2-treated LX-2 cells after the

chase period (Fig. 4D). Consistently, the amount of NEFAs in the incubation media of Lalistat2-treated cells was reduced by 24% (Fig. 4E).

To evaluate findings in LX-2 cells, we performed pulse-chase experiments using primary human HSCs. Similar as observed with LX-2 cells, lipid loading of primary human HSCs led to increased cellular RP content (Fig. 4F). After the 8-h serum-starvation period, the cellular RP content of control HSCs was reduced by 80%, while cellular RP levels of HSCs remained somewhat higher and were decreased by 60% in the presence of Lalistat2 (Fig. 4F).

In summary, the observations of the pulse-chase experiments with human HSC LX-2 cells as well as primary human HSCs indicate that LAL contributes to RE degradation in human HSCs.

3.5 LAL-deficient HSCs accumulate lysosomes and neutral lipids

To more directly investigate the role of LAL in RE degradation of HSCs and to confirm pharmacological studies, we isolated primary HSCs from liver of mice globally lacking LAL by the method of selective detachment [26]. This method involves the cultivation and re-plating of the non-parenchymal cell fraction for two weeks, which yields in almost pure HSC cultures. Laser scanning microscopy of primary LAL-deficient HSCs revealed strong LysoTracker signal as compared to WT HSCs (Fig. 5A), indicative for increased number of lysosomes. Western blot analysis of lysates of primary HSCs for lysosomal marker proteins LAMP1 and RAB7 confirmed increased lysosomal content in HSCs from LAL-ko mice. Protein expression of the stellate cell activation marker α-SMA was higher in LAL-deficient HSCs. Yet, band intensities of the *bona fide* lipid droplet marker protein ADRP were similar between HSC preparations of both genotypes (Fig. 5B). Together, results of staining of cells with LysoTracker and Western blot analyses were indicative for increased lysosomal content of primary LAL-deficient HSCs.

Analyses of cellular neutral lipid content revealed that cultured primary LAL-deficient HSCs contained many-fold higher RP, TG, and total cholesterol levels as compared to cultured primary WT HSCs (Fig. 5C–E). The increase in cellular RP levels was very pronounced since primary WT HSCs had lost all cellular RE content during the two weeks of culture, while LAL-deficient HSCs retained some of cellular REs. (Note: Preliminary measurements gave for non-cultivated, density gradient isolated, primary murine WT and LAL-ko HSCs around 1.9 and 0.6 nmol RP/mg protein, respectively). Next, we performed *in vitro* RE hydrolase activity assays at acidic pH using lysates of primary WT and LAL-ko HSCs. As expected, lysates of LAL-ko HSCs exhibited 90% lower acid RE hydrolase activity as compared to lysates of WT HSCs (Fig. 5F). Furthermore, the addition of Lalistat2 to the assay mixture decreased acid RE hydrolase activity of WT lysates by 78%, while no effect was observed in lysates of LAL-ko HSCs (Fig. 5F). Interestingly, neutral RE hydrolase activity was 25% lower in lysates of LAL-deficient HSCs (Fig. 5G). Addition of the ATGL inhibitor (Ai = Atglistatin) had no effect on RE hydrolase activity of any lysates (Fig. 5G). Addition of HSL inhibitor (76-0079) reduced RE hydrolase activity in lysates of WT HSCs but not of LAL-deficient HSCs, while addition of the serine hydrolase inhibitor Orlistat reduced RE hydrolase activity of lysates of WT and LAL-deficient HSCs (Fig. 5G). Western

blot analyses showed that protein expression levels of HSL and ATGL were lower in primary LAL-deficient as compared to WT HSCs (Fig. 5H). Thus, it was conclusive that lysates of WT HSCs exhibited more ATGL and HSL-dependent RE hydrolase activity as LAL-deficient HSCs.

Together, results of primary LAL-deficient HSCs indicate that, similar as observed in LX-2 lysates, LAL accounts for the majority of acid RE hydrolase activity in primary murine HSCs. Deficiency of LAL in HSCs provokes increased number of lysosomes and accumulation of cellular REs. It can be assumed that REs accumulate in lysosomes, as it has been experimentally demonstrated in hepatocytes [10].

3.6 LAL is not required for the breakdown of REs under serum-starvation

Next, we investigated whether incubation of WT and LAL-deficient primary HSCs with ROH and oleic acid induces lipid droplet formation. Under basal, standard culture conditions of WT and LAL-deficient primary HSCs, the CARS signal of cells (Fig. 6, first column labeled with “Ex. at 816.7 nm + 1064 nm”), as a measure for neutral lipids, was largely overlaid by cellular autofluorescence (Fig. 6, second column labeled with “Ex. 816.7 nm”). As a consequence, most of the CARS signal (depicted in green) when overlaid with autofluorescence signal (depicted in red) turned yellow (Fig. 6, 1st and 3rd panel, third column labeled with “Merge”). However, overnight loading of primary HSCs with ROH and oleic acid induced the formation of round cellular structures, that were visible in the CARS channel (Fig. 6, 2nd and 4th panel, first column) and not overlaid by the autofluorescence signal (Fig. 6, 2nd and 4th panel, third column labeled with “Merge”), consistent with cytosolic lipid droplets. These observations indicate that lipid loading of primary LAL-deficient HSCs, similar as in WT HSCs, induced lipid droplet formation.

To assess the role of LAL in RE degradation of HSCs, we performed pulse-chase experiment using primary HSC preparations from liver of WT and LAL-ko mice. For this, cells were incubated overnight with ROH and oleic acid and chased for 8 h in serum-starvation media (for schematic representation see Fig. 7G). At all time points (before, after lipid loading, and after serum-starvation), cellular RP and, for comparison, TG contents were determined. Consistent with previous measurements of primary murine HSCs (Fig. 5C and D), cellular RP and TG levels of isolated LAL-deficient HSCs were higher as compared to WT HSCs (Fig. 7A and C, “basal”). Loading of WT and LAL-deficient HSCs with ROH and oleic acid similarly increased protein expression level of the lipid droplet marker ADRP in both genotypes (Fig. 7E). Accordingly, cellular RP and TG contents increased to a similar extent (Fig. 7A and C, “loaded”). As a consequence, the absolute amount of RP and TG in LAL-deficient HSCs was higher as compared to WT HSCs. Interestingly, after an 8-h serum-starvation period, cellular RP and TG contents of HSCs of both genotypes declined back close to basal levels (*i.e.* cellular RP and TG contents before lipid loading; Fig. 7A and C, compare “serum-starvation” with “basal”). Calculation of the amount of degraded RP and TG after the chase period revealed no significant difference between the genotypes (Fig. 7B and D). LAL-deficient primary HSCs lost similar amounts of RP during serum-starvation indicating that LAL is not required for this process. Western blot analyses using anti-ADRP antibody confirmed that HSCs of both genotypes similarly lost their cellular lipid droplets.

Detection of RAB7 as lysosomal marker protein showed at all time points more intense bands in preparations of LAL-deficient *vs* WT HSCs (Fig. 7E). To evaluate, if during the starvation period autophagy/lipophagy was induced, we performed Western blot analyses with antibodies specific against autophagy markers ATG7, p62, as well as LC-3B. At all time points, band intensities for the marker proteins ATG7, p62, and LC-3B II were higher in LAL-deficient as compared to WT HSCs (Fig. 7F). More importantly, band intensities of ATG7 and p62 were stronger in cell lysates of serum-starved cells as compared to “basal” or “loaded” cell preparations (Fig. 7F). These increased intensities were consistent with an induction of autophagy. Together, the observations that the amount of degraded RP was similar between WT and LAL-deficient HSCs and that both cell preparations showed induced autophagy, suggest that either LAL is not required for this process or that autophagy/lipophagy overall does not substantially contribute to RE breakdown.

4 Discussion

To date, the rate-limiting enzyme(s) in the breakdown of REs in HSCs is/are unknown. ATGL, PNPLA3, HSL, and LAL have been shown to be expressed in HSCs and to be capable of hydrolyzing REs [10,12,13,37,44,45]. The murine homologue of PNPLA3, however, does not exhibit RE hydrolase activity [13]. Thus, we used the human HSC cell-line LX-2 (homozygous for the I148M variant [21]), primary human HSCs (carrying WT PNPLA3 alleles), and for comparison primary murine HSCs for cell culture experiments. Culturing of HSCs is known to induce activation *per se*, in particular when HSCs are cultured on plastic surfaces [46]. The human HSC cell-line LX-2 has been initially characterized to be similar to activated stellate cells [47]. The activation of the cultured primary HSCs is evident by the expression of α-SMA (Fig. 5B), a marker for stellate cell activation. In contrary, lipid loading (ROH + oleic acid) of LX-2 cells and primary HSCs in the pulse-chase experiments induced the formation of lipid droplets, the expression of *bona fide* lipid droplet protein adipophilin (ADRP, Fig. 7E), and the accumulation of REs (Suppl. Fig. 2B, Figs. 2C, 4B, and 7A), demonstrating that HSCs in our experiments had retained the ability to store REs, a typical feature of the quiescent, *Lrat*-expressing phenotype [48]. It is likely that incubation with ROH to some extent even reverted the activation status of our HSCs into a more quiescent state, since we also observed increased ADRP protein expression levels (Fig. 7E), which has been shown in the past to be inversely regulated to activation markers such as α-SMA, collagen, matrix metalloproteinase-2, or tissue inhibitor of metalloproteinase-1 [15,49,50]. Although we have not investigated the activation status of the HSCs in our experiments in detail (apart from α-SMA expression), culturing of HSCs will certainly lead to their activation. Thus, our results reflect the phenotypical features of activated and not quiescent HSCs and thus need to be interpreted as such.

In this study, we investigated the role of ATGL, PNPLA3, HSL, and LAL in the breakdown of REs of LX-2 cells and primary human HSCs using the small molecule inhibitors R-BEL (for ATGL and PNPLA3), 76-0079 (for HSL), Orlistat (for serine-hydrolases), and Lalistat2 (for LAL). *In vitro* activity assays revealed that ATGL, PNPLA3, HSL, or other serine-hydrolases contribute to a minor extent to *in vitro* neutral RE hydrolase activity of LX-2 cells. In contrast, LAL apparently accounts for the majority of *in vitro* acid RE hydrolysis of LX-2 cells. In pulse-chase experiments, inhibition of ATGL, PNPLA3, HSL, or other serine-

hydrolases, exerted little to no effect on RE degradation. In contrast, inhibition of LAL attenuated RE degradation in the serum-starvation/chase period of LX-2 cells as well as human primary HSCs. However, in similar experiments using primary murine HSCs with genetic deletion of LAL the cellular RE degradation was unaffected, indicating that LAL is not required for RE degradation under serum-starvation.

This study is largely based on the use of inhibitors, what imposes certain limitations of the data interpretation. We used the inhibitors 76-0079 and Lalistat2, which are suggested to be selective for HSL and LAL, respectively [35,51], while the inhibitors R-BEL and Orlistat lack selectivity. R-BEL has been initially developed as calcium-independent phospholipase A2 inhibitor [52] but has later been found to also inhibit human ATGL and PNPLA3 at low μM concentrations [33]. Orlistat, an irreversible inhibitor developed for pancreatic and gastric lipase [53], is nowadays used as more general lipase inhibitor, known to inhibit many lipases including ATGL and HSL [30].

From the effects of the inhibitors we can deduce the following conclusions: (i) The observations that R-BEL neither inhibited *in vitro* RE hydrolase activity nor RE degradation of LX-2 cells and exerted a small effect (25% reduction) on RE degradation of primary human HSCs, indicate that ATGL and PNPLA3 contribute little to RE hydrolase activity or cellular RE degradation of human HSCs under serum-starvation. (ii) A minor contribution of HSL for *in vitro* RE hydrolase activity of LX-2 cells was apparent by using the inhibitor 76-0079, but the same inhibitor exerted no significant effect in pulse-chase experiments. Similarly, also Orlistat inhibited *in vitro* RE hydrolase activity of LX-2 cells but not RE degradation under serum-starvation. These data together indicate that the enzyme(s) limiting for RE hydrolysis of LX-2 cells is/are not inhibited by Orlistat. Furthermore, since Orlistat is known to inhibit ATGL and HSL activity, these enzymes even in combination do not govern RE breakdown of LX-2 cells. (iii) The pronounced inhibitory effect of Lalistat2 on *in vitro* RE hydrolase activity of LX-2 cells as well as on cellular RE loss under serum-starvation indicates that LAL is the major acid RE hydrolase in LX-2 cells, affecting RE homeostasis in these cells. However, the observation that primary murine HSCs, deficient in LAL expression, show comparable RE loss under serum-starvation, suggests that compensatory mechanisms have adopted for LAL-deficiency.

It has to be pointed out that the study was designed to investigate serum-starvation induced RE hydrolysis of cultured human HSCs. PNPLA3 is known to be downregulated upon fasting (in that PNPLA3 is inversely regulated to ATGL [16,17]) and also in our pulse-chase experiments PNPLA3 expression was reduced (Fig. 2B). Thus, the employed experimental setting was inappropriate for investigating the role of PNPLA3 in retinoid metabolism of HSCs. This even more, since we did not add inhibitors during the pulse period, which might have increased RE accumulation when PNPLA3 was inhibited. Furthermore, LX-2 cells are homozygous for the PNPLA3 I148M variant, which is catalytically less active [11]. To circumvent this instance, we have also performed similar pulse-chase experiments with primary human HSCs carrying WT PNPLA3 alleles. In this experiment we observed a 25% attenuation of RE degradation in the presence of R-BEL after serumstarvation (Fig. 2G).

Since R-BEL inhibits both ATGL and PNPLA3, we conclude that these two enzymes, irrespective of the relative contribution, are not limiting for RE hydrolysis under serum-starvation. Hence, even if all inhibitory effect would be fully attributed to one of the enzymes, any of these is apparently essential for RE degradation under serum-starvation. However, these results do not rule out that under normo-physiological conditions PNPLA3 might play a role in RE homeostasis of the liver.

In the past, the role of ATGL in RE degradation has been studied in primary murine HSCs by Taschler et al. [13]. In agreement with our study, they observed in *in vitro* hydrolase activity assays using WT and ATGL-ko non-parenchymal cell preparations (containing the HSC fraction) that ATGL contributes to *in vitro* RE hydrolase activity of HSCs. In their study, prolonged inhibition of ATGL in primary WT HSCs with the small molecule inhibitor Atglistatin® led to an accumulation of cellular RE content. Furthermore, primary ATGL-deficient HSCs showed attenuated RE degradation under serum-starvation. In the present study, we used R-BEL to inhibit human ATGL as the ATGL-specific inhibitor Atglistatin® has not been found to inhibit human ATGL [30]. Interestingly, in pulse-chase experiments with LX-2 cells, we observed no effect of R-BEL on cellular RE degradation upon serum-starvation. A possible explanation for this seeming discrepancy with attenuated RE loss of ATGL-deficient primary murine HSCs, as reported by Taschler et al. [13] could be that ATGL-deficient HSCs “chronically” lack ATGL activity and as a consequence exhibit much higher cellular RE and, importantly, TG levels. TG is known to compete as substrate for RE hydrolysis [13], a mechanism expected to slow down RE hydrolysis. In our study, we inhibited ATGL “acutely” during the serum-starvation period, so that lipid loading of LX-2 cells was not affected, and cells contained similar cellular RE/TG contents at the start of the serum-starvation period. Interestingly, Tuohetahuntila et al. [44] reported that primary, ATGL-deficient HSCs showed same loss of cellular REs as WT HSCs during a culture period after isolation, also arguing for a non-limiting role of ATGL in RE hydrolysis. In accordance with this view, ATGL-deficient mice do not exhibit alterations in circulating ROH or hepatic RE content [13].

HSL-ko mice exhibit manifold increased RE content in white adipose tissue, clearly demonstrating a rate-limiting role in RE hydrolysis [12,13]. In liver, however, HSL has been thought for some time not to be expressed [54]. One report on a limiting role of HSL in hepatic cholesteryl ester hydrolysis [55] demonstrated that HSL is expressed in liver where it plays a functional role. More recently, liver HSL expression was shown to be higher in parenchymal cells than in stellate cells [14,55]. While HSL expression has been demonstrated in human LX-2 and primary rat HSCs [37], no expression was detected in murine HSCs [22]. In our study, we could confirm the expression of HSL in LX-2 cells. Furthermore, employing an HSL-specific inhibitor, we observed minor inhibition of *in vitro* RE hydrolase activity and no effect on cellular RE degradation of LX-2 cells. Thus, our findings indicate that HSL is not limiting in RE metabolism of LX-2 cells. For comparison, Shajari et al. [37] recently reported that isoproterenol stimulation of primary rat HSCs induces HSL phosphorylation which was accompanied by decreased ORO staining and decreased vitamin A autofluorescence of cells. Authors concluded that HSL participates in RE hydrolysis of HSCs, what we could not confirm in our study. Furthermore, the study by Shajari et al. [37] reported that expression of HSL in HSCs is lost upon activation. This

observation is intriguing and may explain why under some conditions (*e.g.* activated HSCs with increased α-SMA expression), HSL expression may not be detectable. However, the phenotype of HSL-ko mice, which shows no alterations in hepatic RE content nor circulating ROH levels, even when fed a vitamin A-deficient diet [13], demonstrates that HSL is not limiting for RE hydrolysis in liver.

In this study we also examined the hypothesis that RE degradation of HSCs might be a redundant system [56] and several RE hydrolases act in concert in controlling RE hydrolysis. For this we used the unspecific serine-hydrolase/lipase inhibitor Orlistat. Orlistat has been shown in *in vitro* activity assays to inhibit human ATGL and HSL [30], carboxyl esterase 2 [57], as well as LAL [58,59] in the low and sub μM range, respectively. Thus, we expected that Orlistat might effectively inhibit *in vitro* RE hydrolase activity and/or cellular RE degradation. In fact, addition of Orlistat inhibited *in vitro* neutral RE hydrolase activity of LX-2 cell lysates to a degree comparable to the sum of the inhibitory effect of ATGL, PNPLA3, and HSL inhibition (*i.e.* R-BEL and 76-0079). However, still > 50% of neutral RE hydrolase activity was not inhibited by Orlistat and was only lost after heat inactivation (Fig. 1C). The observation, however, that Orlistat exerted virtually no effect on cellular RE degradation under serum-starvation indicated that even the combined inhibition of ATGL, PNPLA3, and HSL as well as potentially other serine-hydrolases does not affect cellular RE levels under serum-starvation. This suggests that RE degradation of HSC LX-2 cells is under the control of (a) non-Orlistat-inhibitable hydrolase(s).

Several studies demonstrated a role of autolysosomal hydrolysis of lipid droplet-associated neutral lipids (=lipophagy) in HSCs [8,60–62]. In our study, we observed that the majority of acid RE hydrolase activity, measured in an, for LAL optimized, activity assay, can be attributed to LAL, since the presence of Lalistat2 almost completely abolished hydrolytic activity. This might be also caused by the activation of the HSCs, since autophagy and also LAL expression are known to be induced upon stellate cell activation [45,61]. Furthermore, acid *in vitro* RE hydrolase activity of LX-2 cells was stimulated by the presence of negatively charged phospholipids, a characteristic feature of LAL activity [42]. Comparable observations, that LAL is responsible for the majority of acid RE hydrolase activity, have been reported by Tuohe-tahuntila et al. [45] for rat primary HSCs. Furthermore, in our study, inhibition of LAL in pulse-chase experiments using LX-2 cells attenuated RE degradation. In contrast, in similar pulse-chase experiments using primary murine LAL-deficient HSCs, the loss of cellular RE content was not affected. For comparison, Tuohetahuntila et al. [45] observed that primary rat HSCs, cultured with delipidated serum and in the presence of Lalistat2 for seven days, were defective in degrading cellular REs as compared to control cells. These somewhat different outcomes of the Lalistat2 inhibitor experiments (of this study and Tuohetahuntila et al. [45]) in comparison to functional RE degradation of LAL-deficient primary HSCs (of this study), questions whether under these different experimental conditions, lipid loading induced the formation of cytosolic lipid droplets and whether serum-starvation induced autophagosome formation? These questions arise since the lack of LAL activity is expected to associate with impaired lipophagy. Lipid loading of cells with defective lipophagy could therefore result in the accumulation of neutral lipids in autolysosomes (*via* lipophagy of cytosolic lipid droplets) rather than cytosolic lipid droplets. We and others [45] have investigated the formation of cytosolic lipid droplets by live-cell

imaging, the pre-existence of cytosolic lipid droplets and the increase of their number upon lipid loading. In our study, we further observed by Western blotting that after serum-starvation, the protein levels of the *bona fide* lipid droplet marker protein perilipin 2/adipophilin/ADRP [63] dropped below detection limit, indicating that cytosolic lipid droplets have been degraded. Furthermore, LAL-deficient HSCs *per se* showed more intense bands for ATG7, p62, and LC-3B II, which further increased upon serum-starvation, altogether indicative for increased autophagosomal content and induction of autophagy. Together, these observations indicate that lipid loading of LAL-deficient primary HSCs induced cytosolic lipid droplet formation, which were degraded upon serum-starvation. Elevated marker proteins for autophagy are indicative for increased autophagosomal content but may not necessarily be indicative for increased autophagosomal activity. Thus, it is conclusive that despite defective autophagosomal neutral lipid processing, RE degradation upon serum-starvation does not require the activity of LAL. The contradicting observation in LX-2 cells, which showed attenuated cellular RE hydrolysis upon acute LAL inhibition under serum-starvation, may indicate species differences. Yet, chronic but not acute LAL-deficiency may induce compensatory mechanisms, involving alternative lysosomal activities that at least in part facilitate RE degradation in lysosomes. Similar mechanisms have been suggested for lysosomal clearance of TGs [22]. Alternatively, the observation that Lalistat2 treatment attenuates cellular RE degradation upon serum-starvation could be a consequence of unspecific inhibition of additional enzymes involved in RE hydrolysis.

Several studies have shown that the inhibition of autophagy in HSCs leads to a delay in stellate cell activation and the development of liver fibrosis, which is associated with the loss of neutral lipid stores [45,60,61]. Inhibition of autophagy, either pharmacologically or by *atg5* or *atg7* knockdown, induced increased TG content, increased number of lipid droplets, and increased ADRP protein levels [61]. Furthermore, a colocalization of lipid droplets and LC3-B was observed upon activation [60], suggesting that autophagy/lipophagy is induced in activated stellate cells and drives loss of lipid droplets. In our study on LAL-deficient HSCs, we observed increased RAB7 and LAMP1 protein content and positive staining with LysoTracker, which is consistent with defective lysosomal clearance. Increased cellular TG, RE, and total cholesterol contents are apparently consequences of this defect. These increased cellular neutral lipids are presumably contained in lysosomal particles and not accessible for further metabolization, even after serum-starvation.

The observation that primary HSCs of LAL-deficient mice contained increased neutral lipid content, including REs, is conflicting with the vitamin A phenotype of mice globally lacking LAL. These animals exert decreased hepatic RE levels, but rather increased hepatic TG levels [10,45]. This discrepancy, however, could be explained by the observation that livers of LAL-ko mice show increased stellate cell activation, which would induce a loss of cellular RE stores. This hypothesis appears plausible since humans suffering cholesteryl ester storage disease frequently show signs of liver fibrosis [64].

Collectively, results of this study suggest that in cultured human HSCs, as it can also be concluded from knockout-mouse models, ATGL, PNPLA3, HSL, nor LAL play a limiting role in RE degradation of HSCs. Apparently, the rate-limiting enzyme(s) is/are non-

inhibitable by Orlistat. Future studies are required to unravel the identity of this/these enzyme(s).

Supplementary Material

Refer to Web version on PubMed Central for supplementary material.

Acknowledgments/grant support

This work was supported by the Leuchtturmprojekt/Flagship Project “Lipases and Lipid Signaling” (A.L., R.Z.), funded by BioTechMed-Graz, Austria. Further support was received by the grants I3535 (A.L.), P31638 (U.T.), F7310-B21 (M.T.), and DK Molecular Enzymology FWF/W9 (R.Z.), funded by the Austrian Science Fund (FWF), Austria, and DOC fellowship 25049 (L.P.), funded by the Austrian Academy of Sciences (OEAW), Austria. Imaging was performed at the IMB-Graz Microscopy Core Facility. We acknowledge the support of the field of excellence BioHealth. We thank Dagmar Kratky (Gottfried Schatz Research Center for Cell Signaling, Metabolism and Aging, Molecular Biology) for sharing Lipa$^{tm1a(EUCOMM)Hmgu}$ mice.

Abbreviations

ABHD5	α/β hydrolase domain-containing protein 5
ADRP	adipose differentiation-related protein
α-SMA	α-smooth muscle actin
ATG7	autophagy related 7
ATGL	adipose triglyceride lipase
BSA	bovine serum albumin
CARS	coherent anti-Stokes Raman scattering
CGI-58	comparative gene identification-58
CHOL	cholesterol
DMSO	dimethyl sulfoxide
FA	fatty acid
FCS	fetal calf serum
FD	fluorescence detection
GAPDH	glyceraldehyde 3-phosphate dehydrogenase
HPLC	high-performance liquid chromatography
HSC	hepatic stellate cell
HSL	hormone-sensitive lipase
LAL	lysosomal acid lipase
LAMP1	lysosomal-associated membrane protein 1

Europe PMC Funders Author Manuscripts

Europe PMC Funders Author Manuscripts

LC-3B	microtubule-associated protein 1B-light chain 3
LIPA	lipase A = LAL
LIPE	lipase E = HSL
ko	knockout
NEFA	non-esterified fatty acid
PC	phosphatidylcholine
PI	phosphatidylinositol
PMSF	phenylmethylsulfonylfluoride
PNPLA2	patatin-like phospholipase domain-containing 2 = ATGL
PNPLA3	patatin-like phospholipase domain-containing 3
RAB7	ras-related protein 7
R-BEL	(*R*)-Bromoenol lactone
RE	retinyl ester
ROH	retinol
RP	retinyl palmitate
S.D.	standard deviation
SMT	SUMO-tag
TG	triglyceride
WT	wild-type
36B4	acidic ribosomal phosphoprotein P0

References

[1]. Friedman SL. Hepatic stellate cells : protean, multifunctional, and enigmatic cells of the liver. Physiol Rev. 2008; 88:125–172. DOI: 10.1152/physrev.00013.2007 [PubMed: 18195085]

[2]. Blaner WS, O'Byrne SM, Wongsiriroj N, Kluwe J, D'Ambrosio DM, Jiang H, Schwabe RF, Hillman EMC, Piantedosi R, Libien J. Hepatic stellate cell lipid droplets: a specialized lipid droplet for retinoid storage. Biochim Biophys Acta. 2009; 1791:467–473. DOI: 10.1016/j.bbalip.2008.11.001 [PubMed: 19071229]

[3]. Green MH, Green JB, Berg T, Norum KR, Blomhoff R. Changes in hepatic parenchymal and nonparenchymal cell vitamin A content during vitamin A depletion in the rat. J Nutr. 1988; 118:1331–1335. DOI: 10.1093/jn/118.11.1331 [PubMed: 3193250]

[4]. Bankson DD, Ellis JK, Russell RM. Effects of a vitamin-A-free diet on tissue vitamin A concentration and dark adaptation of aging rats. Exp Gerontol. 1989; 24:127–136. DOI: 10.1016/0531-5565(89)90023-5 [PubMed: 2721601]

[5]. Zhang C-Y, Yuan W-G, He P, Lei J-H, Wang C-X. Liver fibrosis and hepatic stellate cells: etiology, pathological hallmarks and therapeutic targets. World J Gastroenterol. 2016; 22:10512–10522. DOI: 10.3748/wjg.v22.i48.10512 [PubMed: 28082803]

[6]. Lemoinne S, Cadoret A, El Mourabit H, Thabut D, Housset C. Origins and functions of liver myofibroblasts. Biochim Biophys Acta Mol Basis Dis. 2013; 1832:948–954. DOI: 10.1016/J.BBADIS.2013.02.019

[7]. Martinez-Lopez N, Singh R. Autophagy and lipid droplets in the liver. Annu Rev Nutr. 2015; 35:215–237. DOI: 10.1146/annurev-nutr-071813-105336 [PubMed: 26076903]

[8]. Singh R, Kaushik S, Wang Y, Xiang Y, Novak I, Komatsu M, Tanaka K, Cuervo AM, Czaja MJ. Autophagy regulates lipid metabolism. Nature. 2009; 458:1131–1135. DOI: 10.1038/nature07976 [PubMed: 19339967]

[9]. Du H, Duanmu M, Witte D, Grabowski GA. Targeted disruption of the mouse lysosomal acid lipase gene: long-term survival with massive cholesteryl ester and triglyceride storage. Hum Mol Genet. 1998; 7:1347–1354. DOI: 10.1093/hmg/7.9.1347 [PubMed: 9700186]

[10]. Grumet L, Eichmann TO, Taschler U, Zierler KAKA, Leopold C, Moustafa T, Radovic B, Romauch M, Yan C, Du H, Haemmerle G, et al. Lysosomal acid lipase hydrolyzes retinyl ester and affects retinoid turnover. J Biol Chem. 2016; 291:17977–17987. DOI: 10.1074/jbc.M116.724054 [PubMed: 27354281]

[11]. Pirazzi C, Valenti L, Motta BM, Pingitore P, Hedfalk K, Mancina RM, Burza MA, Indiveri C, Ferro Y, Montalcini T, Maglio C, et al. PNPLA3 has retinyl-palmitate lipase activity in human hepatic stellate cells. Hum Mol Genet. 2014; 23:4077–4085. DOI: 10.1093/hmg/ddu121 [PubMed: 24670599]

[12]. Ström K, Gundersen TE, Hansson O, Lucas S, Fernandez C, Blomhoff R, Holm C, Strom K, Gundersen TE, Hansson O, Lucas S, et al. Hormone-sensitive lipase (HSL) is also a retinyl ester hydrolase: evidence from mice lacking HSL. FASEB J. 2009; 23:2307–2316. DOI: 10.1096/fj.08-120923 [PubMed: 19246492]

[13]. Taschler U, Schreiber R, Chitraju C, Grabner GF, Romauch M, Wolinski H, Haemmerle G, Breinbauer R, Zechner R, Lass A, Zimmermann R. Adipose triglyceride lipase is involved in the mobilization of triglyceride and retinoid stores of hepatic stellate cells. Biochim Biophys Acta. 2015; 1851:937–945. DOI: 10.1016/j.bbalip.2015.02.017 [PubMed: 25732851]

[14]. Mello T, Nakatsuka A, Fears S, Davis W, Tsukamoto H, Bosron WF, Sanghani SP, Vita A. Expression of carboxylesterase and lipase genes in rat liver cell-types. Biochem Biophys Res Commun. 2008; 374:460–464. DOI: 10.1016/j.bbrc.2008.07.024 [PubMed: 18639528]

[15]. Hong Y, Li S, Wang J, Li Y. In vitro inhibition of hepatic stellate cell activation by the autophagy-related lipid droplet protein ATG2A. Sci Rep. 2018; 8doi: 10.1038/s41598-018-27686-6

[16]. Lake AC, Sun Y, Li J-L, Kim JE, Johnson JW, Li D, Revett T, Shih HH, Liu W, Paulsen JE, Gimeno RE. Expression, regulation, and triglyceride hydrolase activity of Adiponutrin family members. J Lipid Res. 2005; 46:2477–2487. DOI: 10.1194/jlr.M500290-JLR200 [PubMed: 16150821]

[17]. Huang Y, He S, Li JZ, Seo Y-K, Osborne TF, Cohen JC, Hobbs HH. A feed-forward loop amplifies nutritional regulation of PNPLA3. Proc Natl Acad Sci U S A. 2010; 107:7892–7897. DOI: 10.1073/pnas.1003585107 [PubMed: 20385813]

[18]. Bruschi FV, Claudel T, Tardelli M, Caligiuri A, Stulnig TM, Marra F, Trauner M. The PNPLA3 I148M variant modulates the fibrogenic phenotype of human hepatic stellate cells. Hepatology. 2017; 65:1875–1890. DOI: 10.1002/hep.29041 [PubMed: 28073161]

[19]. Pingitore P, Romeo S. The role of PNPLA3 in health and disease. Biochim Biophys Acta Mol Cell Biol Lipids. 2019; 1864:900–906. DOI: 10.1016/j.bbalip.2018.06.018 [PubMed: 29935383]

[20]. Kovarova M, Königsrainer I, Königsrainer A, Machicao F, Häring H-U, Schleicher E, Peter A. The genetic variant I148M in *PNPLA3* is associated with increased hepatic retinyl-palmitate storage in humans. J Clin Endocrinol Metab. 2015; 100:E1568–E1574. DOI: 10.1210/jc.2015-2978 [PubMed: 26439088]

[21]. Pingitore P, Sasidharan K, Ekstrand M, Prill S, Lindén D, Romeo S. Human multilineage 3D spheroids as a model of liver steatosis and fibrosis. Int J Mol Sci. 2019; 20doi: 10.3390/ijms20071629

[22]. Pajed L, Wagner C, Taschler U, Schreiber R, Kolleritsch S, Fawzy N, Pototschnig I, Schoiswohl G, Pusch L-M, Wieser BI, Vesely P, et al. Hepatocyte-specific deletion of lysosomal acid lipase leads to cholesteryl ester but not triglyceride or retinyl ester accumulation. J Biol Chem. 2019; 294:9118–9133. DOI: 10.1074/jbc.RA118.007201 [PubMed: 31023823]

[23]. Haemmerle G, Zimmermann R, Hayn M, Theussl C, Waeg G, Wagner EFE, Sattler W, Magin TM, Zechner R. Hormone-sensitive lipase deficiency in mice causes diglyceride accumulation in adipose tissue, muscle, and testis. J Biol Chem. 2002; 277:4806–4815. DOI: 10.1074/jbc.M110355200 [PubMed: 11717312]

[24]. Bruschi FV, Claudel T, Tardelli M, Starlinger P, Marra F, Trauner M. PNPLA3 I148M variant impairs liver×receptor signaling and cholesterol homeostasis in human hepatic stellate cells. Hepatol Commun. 2019; 3:1191–1204. DOI: 10.1002/hep4.1395 [PubMed: 31497741]

[25]. Blomhoff R, Berg T. Isolation and cultivation of rat liver stellate cells. Methods Enzymol. 1990; 190:58–71. DOI: 10.1016/0076-6879(90)90009-P [PubMed: 1965004]

[26]. Schreiber R, Taschler U, Wolinski H, Seper A, Tamegger SN, Graf M, Kohlwein SD, Haemmerle G, Zimmermann R, Zechner R, Lass A. Esterase 22 and beta-glucuronidase hydrolyze retinoids in mouse liver. J Lipid Res. 2009; 50:2514–2523. DOI: 10.1194/jlr.M000950 [PubMed: 19723663]

[27]. Jaeger D, Schoiswohl G, Hofer P, Schreiber R, Schweiger M, Eichmann TO, Pollak NMNM, Poecher N, Grabner GFGF, Zierler KAKA, Eder S, et al. Fasting-induced G0/G1 switch gene 2 and FGF21 expression in the liver are under regulation of adipose tissue derived fatty acids. J Hepatol. 2015; 63:437–445. DOI: 10.1016/j.jhep.2015.02.035 [PubMed: 25733154]

[28]. Schweiger, M, Eichmann, TO, Taschler, U, Zimmermann, R, Zechner, R, Lass, A. Measurement of Lipolysis. 1st ed. Elsevier Inc; Burlington: 2014.

[29]. Nomura DK, Casida JE. Lipases and their inhibitors in health and disease. Chem Biol Interact. 2016; 259:211–222. DOI: 10.1016/j.cbi.2016.04.004 [PubMed: 27067293]

[30]. Iglesias J, Lamontagne J, Erb H, Gezzar S, Zhao S, Joly E, Truong VL, Skorey K, Crane S, Madiraju SRM, Prentki M. Simplified assays of lipolysis enzymes for drug discovery and specificity assessment of known inhibitors. J Lipid Res. 2016; 57:131–141. DOI: 10.1194/jlr.D058438 [PubMed: 26423520]

[31]. Lass A, Zimmermann R, Haemmerle G, Riederer M, Schoiswohl G, Schweiger M, Kienesberger P, Strauss JG, Gorkiewicz G, Zechner R. Adipose triglyceride lipase-mediated lipolysis of cellular fat stores is activated by CGI-58 and defective in Chanarin-Dorfman syndrome. Cell Metab. 2006; 3:309–319. DOI: 10.1016/j.cmet.2006.03.005 [PubMed: 16679289]

[32]. Wang Y, Kory N, BasuRay S, Cohen JC, Hobbs HH. PNPLA3, CGI-58, and inhibition of hepatic triglyceride hydrolysis in mice. Hepatology. 2019; 69:2427–2441. DOI: 10.1002/hep.30583 [PubMed: 30802989]

[33]. Jenkins CM, Mancuso DJ, Yan W, Sims HF, Gibson B, Gross RW. Identification, cloning, expression, and purification of three novel human calcium-independent phospholipase A2 family members possessing triacylglycerol lipase and acylglycerol transacylase activities. J Biol Chem. 2004; 279:48968–48975. DOI: 10.1074/jbc.M407841200 [PubMed: 15364929]

[34]. Chung C, Doll JA, Gattu AK, Shugrue C, Cornwell M, Fitchev P, Crawford SE. Anti-angiogenic pigment epithelium-derived factor regulates hepatocyte triglyceride content through adipose triglyceride lipase (ATGL). J Hepatol. 2008; 48:471–478. DOI: 10.1016/j.jhep.2007.10.012 [PubMed: 18191271]

[35]. Ebdrup S, Refsgaard HHF, Fledelius C, Jacobsen P. Synthesis and structure–-activity relationship for a novel class of potent and selective carbamate-based inhibitors of hormone selective lipase with acute in vivo antilipolytic effects. J Med Chem. 2007; 50:5449–5456. DOI: 10.1021/jm0607653 [PubMed: 17918819]

[36]. James GT. Inactivation of the protease inhibitor phenylmethylsulfonyl fluoride in buffers. Anal Biochem. 1978; 86:574–579. DOI: 10.1016/0003-2697(78)90784-4 [PubMed: 26289]

[37]. Shajari S, Saeed A, Smith-Cortinez NF, Heegsma J, Sydor S, Faber KN. Hormone-sensitive lipase is a retinyl ester hydrolase in human and rat quiescent hepatic stellate cells, Biochim. Biophys. Acta Mol Cell Biol Lipids. 2019; 1864:1258–1267. DOI: 10.1016/j.bbalip.2019.05.012

[38]. Zimmermann R, Strauss JGJG, Haemmerle G, Schoiswohl G, Birner-Gruenberger R, Riederer M, Lass A, Neuberger G, Eisenhaber F, Hermetter A, Zechner R. Fat mobilization in adipose tissue is promoted by adipose triglyceride lipase. Science (80-.). 2004; 306:1383–1386. DOI: 10.1126/science.1100747

[39]. Pingitore P, Pirazzi C, Mancina RM, Motta BM, Indiveri C, Pujia A, Montalcini T, Hedfalk K, Romeo S. Recombinant PNPLA3 protein shows triglyceride hydrolase activity and its I148M mutation results in loss of function. Biochim Biophys Acta. 2014; 1841:574–580. DOI: 10.1016/j.bbalip.2013.12.006 [PubMed: 24369119]

[40]. Fredrikson G, Stralfors P, Nilsson NO, Belfrage P, Strålfors P, Nilsson NO, Belfrage P. Hormone-sensitive lipase of rat adipose tissue. Purification and some properties. J Biol Chem. 1981; 256:6311–6320. [PubMed: 7240206]

[41]. Gruber A, Cornaciu I, Lass A, Schweiger M, Poeschl M, Eder C, Kumari M, Schoiswohl G, Wolinski H, Kohlwein SD, Zechner R, et al. The N-terminal region of comparative gene identification-58 (CGI-58) is important for lipid droplet binding and activation of adipose triglyceride lipase. J Biol Chem. 2010; 285doi: 10.1074/jbc.M109.064469

[42]. Joutti A, Vainio P, Brotherus JR, Paltauf F, Kinnunen PK. The active site and the phospholipid activation of rat liver lysosomal lipase are not stereospecific. Chem Phys Lipids. 1981; 29:235–239. DOI: 10.1016/0009-3084(81)90054-2 [PubMed: 7296725]

[43]. Hamilton J, Jones I, Srivastava R, Galloway P. A new method for the measurement of lysosomal acid lipase in dried blood spots using the inhibitor Lalistat 2. Clin Chim Acta. 2012; 413:1207–1210. DOI: 10.1016/j.cca.2012.03.019 [PubMed: 22483793]

[44]. Tuohetahuntila M, Molenaar MR, Spee B, Brouwers JF, Houweling M, Vaandrager AB, Helms JB. ATGL and DGAT1 are involved in the turnover of newly synthesized triacylglycerols in hepatic stellate cells. J Lipid Res. 2016; doi: 10.1194/jlr.M066415

[45]. Tuohetahuntila M, Molenaar MR, Spee B, Brouwers JF, Wubbolts R, Houweling M, Yan C, Du H, VanderVen BC, Vaandrager AB, Helms JB. Lysosome-mediated degradation of a distinct pool of lipid droplets during hepatic stellate cell activation. J Biol Chem. 2017; 292:12436–12448. DOI: 10.1074/jbc.M117.778472 [PubMed: 28615446]

[46]. De Margreet Leeuw A, Mccarthy SP, Geerts A, Knook DL. Purified rat liver fat-storing cells in culture divide and contain collagen. Hepatology. 1984; 4:392–403. DOI: 10.1002/hep.1840040307 [PubMed: 6373550]

[47]. Xu L, Hui aY, Albanis E, Arthur MJ, O'Byrne SM, Blaner WS, Mukherjee P, Friedman SL, Eng FJ. Human hepatic stellate cell lines, LX-1 and LX-2: new tools for analysis of hepatic fibrosis. Gut. 2005; 54:142–151. DOI: 10.1136/gut.2004.042127 [PubMed: 15591520]

[48]. Kluwe J, Wongsiriroj N, Troeger JS, Gwak G, Dapito DH, Pradere J, Jiang H, Siddiqi M, Piantedosi R, Byrne SMO, Blaner WS, et al. Absence of Hepatic Stellate Cell Retinoid Lipid Droplets Does Not Enhance Hepatic Fibrosis but Decreases Hepatic Carcinogenesis. 2011; :1–10. DOI: 10.1136/gut.2010.209551

[49]. El Taghdouini A, Najimi M, Sancho-Bru P, Sokal E, van Grunsven LA. In vitro reversion of activated primary human hepatic stellate cells. Fibrogenesis Tissue Repair. 2015; 8doi: 10.1186/s13069-015-0031-z

[50]. Lee TF, Mak KM, Rackovsky O, Lin Y-L, Kwong AJ, Loke JC, Friedman SL. Downregulation of hepatic stellate cell activation by retinol and palmitate mediated by adipose differentiation-related protein (ADRP). J Cell Physiol. 2010; 223:648–657. DOI: 10.1002/jcp.22063 [PubMed: 20143336]

[51]. Rosenbaum AI, Cosner CC, Mariani CJ, Maxfield FR, Wiest O, Helquist P. Thiadiazole carbamates: potent inhibitors of lysosomal acid lipase and potential Niemann-Pick type C disease therapeutics. J Med Chem. 2010; 53:5281–5289. DOI: 10.1021/jm100499s [PubMed: 20557099]

[52]. Jenkins CM, Han X, Mancuso DJ, Gross RW. Identification of calcium-independent phospholipase A2 (iPLA2) beta, and not iPLA2gamma, as the mediator of arginine vasopressin-induced arachidonic acid release in A-10 smooth muscle cells. Enantioselective mechanism-based discrimination of mammalian iPLA2s. J Biol Chem. 2002; 277:32807–32814. DOI: 10.1074/jbc.M202568200 [PubMed: 12089145]

[53]. Heck AM, Yanovski JA, Calis KA. Orlistat, a new lipase inhibitor for the management of obesity. Pharmacotherapy. 2000; 20:270–279. DOI: 10.1592/phco.20.4.270.34882 [PubMed: 10730683]

[54]. Holm C, Belfrage P, Fredrikson G. Immunological evidence for the presence of hormone-sensitive lipase in rat tissues other than adipose tissue. Biochem Biophys Res Commun. 1987; 148:99–105. DOI: 10.1016/0006-291X(87)91081-3 [PubMed: 3675597]

[55]. Sekiya M, Osuga J-I, Yahagi N, Okazaki H, Tamura Y, Igarashi M, Takase S, Harada K, Okazaki S, Iizuka Y, Ohashi K, et al. Hormone-sensitive lipase is involved in hepatic cholesteryl ester hydrolysis. J Lipid Res. 2008; 49:1829–1838. DOI: 10.1194/jlr.M800198-JLR200 [PubMed: 18480494]

[56]. Haemmerle G, Lass A. Genetically modified mouse models to study hepatic neutral lipid mobilization. Biochim Biophys Acta, Mol Basis Dis. 2018; doi: 10.1016/j.bbadis.2018.06.001

[57]. Xiao D, Shi D, Yang D, Barthel B, Koch TH, Yan B. Carboxylesterase-2 is a highly sensitive target of the antiobesity agent orlistat with profound implications in the activation of anticancer prodrugs. Biochem Pharmacol. 2013; 85:439–447. DOI: 10.1016/j.bcp.2012.11.026 [PubMed: 23228697]

[58]. Rosenbaum AI, Rujoi M, Huang AY, Du H, Grabowski GA, Maxfield FR. Chemical screen to reduce sterol accumulation in Niemann-Pick C disease cells identifies novel lysosomal acid lipase inhibitors. Biochim Biophys Acta. 2009; 1791:1155–1165. DOI: 10.1016/j.bbalip.2009.08.005 [PubMed: 19699313]

[59]. Du H, Sheriff GA, Du S, Grabowski H, Du H, Sheriff GA, Du S, Grabowski H. Characterization of lysosomal acid lipase by site-directed mutagenesis and heterologous expression. J Biol Chem. 1995; 270:27766–27772. DOI: 10.1074/jbc.270.46.27766 [PubMed: 7499245]

[60]. Thoen LFR, Guimarães ELM, Dollé L, Mannaerts I, Najimi M, Sokal E, van Grunsven La. A role for autophagy during hepatic stellate cell activation. J Hepatol. 2011; 55:1353–1360. DOI: 10.1016/j.jhep.2011.07.010 [PubMed: 21803012]

[61]. Hernández-Gea V, Ghiassi-Nejad Z, Rozenfeld R, Gordon R, Fiel MI, Yue Z, Czaja MJ, Friedman SL. Autophagy releases lipid that promotes fibrogenesis by activated hepatic stellate cells in mice and in human tissues. Gastroenterology. 2012; 142:938–946. DOI: 10.1053/j.gastro.2011.12.044 [PubMed: 22240484]

[62]. Chen M, Liu J, Yang W, Ling W. Lipopolysaccharide mediates hepatic stellate cell activation by regulating autophagy and retinoic acid signaling. Autophagy. 2017; 13:1813–1827. DOI: 10.1080/15548627.2017.1356550 [PubMed: 29160747]

[63]. Straub BK, Stoeffel P, Heid H, Zimbelmann R, Schirmacher P. Differential pattern of lipid droplet-associated proteins and de novo perilipin expression in hepatocyte steatogenesis. Hepatology. 2008; 47:1936–1946. DOI: 10.1002/hep.22268 [PubMed: 18393390]

[64]. Bernstein DL, Hülkova H, Bialer MG, Desnick RJ. Cholesteryl ester storage disease: review of the findings in 135 reported patients with an underdiagnosed disease. J Hepatol. 2013; 58:1230–1243. DOI: 10.1016/J.JHEP.2013.02.014 [PubMed: 23485521]

Europe PMC Funders Author Manuscripts

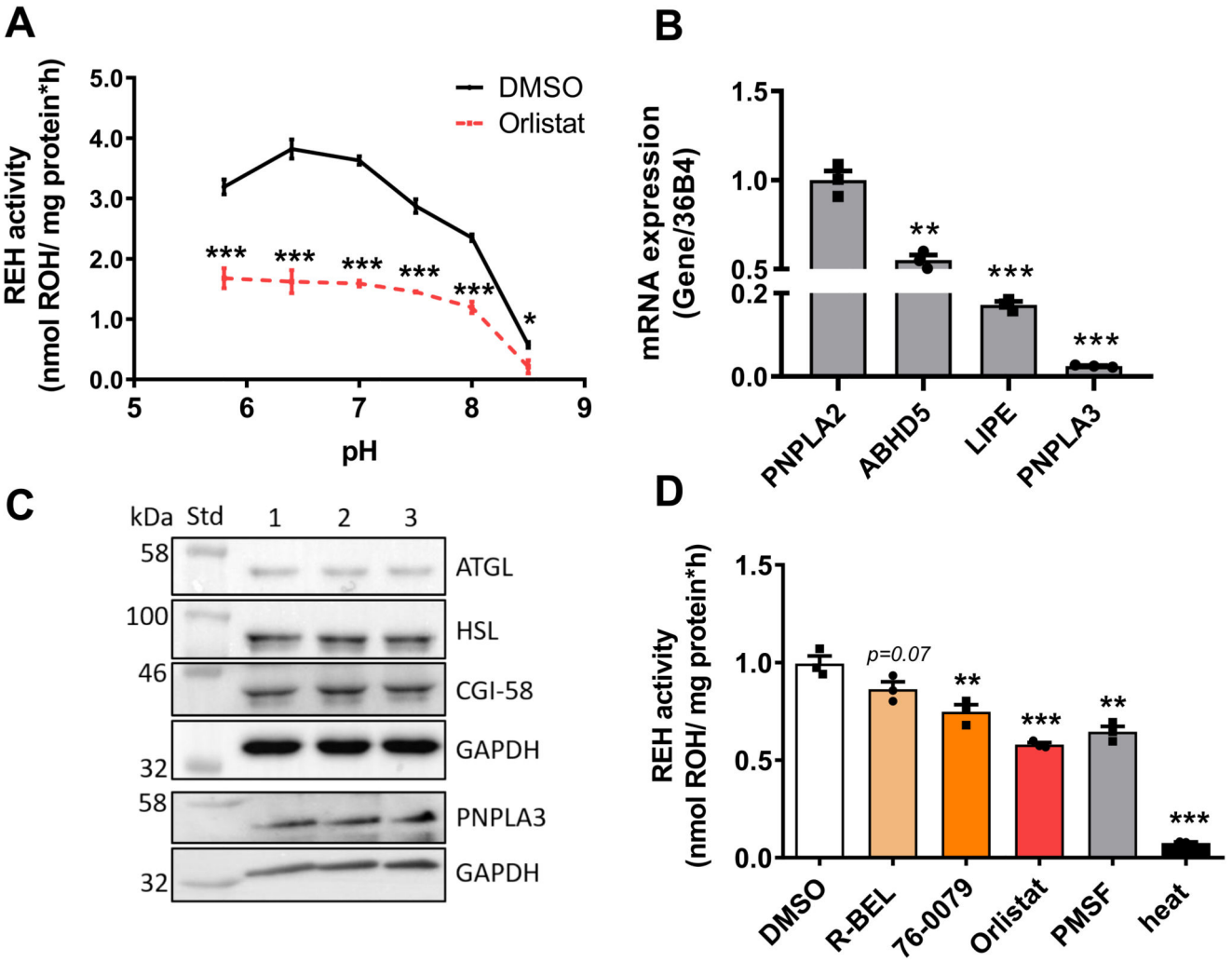

Fig. 1. Neutral RE hydrolase activity of human HSC cell-line LX-2 is partially inhibited by Orlistat.

(A) Cell lysates of LX-2 cells (1000 × *g* supernatant) were incubated with RP (150 μM) as substrate for 1 h at 37 °C. Incubation mixtures contained either Orlistat (20 μM) or DMSO as control. Substrate was emulsified with PC (150 μM). Bis-Tris propane buffers of different pH were added to the mixture for adjusting different pH values as indicated. Retinoids were *n*-hexane extracted and ROH content was analyzed by HPLC-FD. (B) Isolated RNA was transcribed and gene expression of *PNPLA2* (=ATGL), *ABHD5* (=CGI-58), *LIPE* (=HSL), and *PNPLA3* were determined by qPCR. Expression levels were calculated by the ΔΔCT method using *36B4* as housekeeping gene with *PNPLA2* expression arbitrarily set to 1. (C) Protein expression of ATGL, CGI-58, HSL, and PNPLA3 in LX-2 cells was determined by Western blot analyses using specific antibodies. 1, 2, and 3 indicate independent cell lysate preparations of LX-2 cells. Anti-GAPDH antibody was used as loading control. (D) Cell lysates of LX-2 cells were incubated with RP as substrate (at pH 7.5) as described in A. Small molecule inhibitors were added to the mixtures as indicated: DMSO (= control), R-BEL (20 μM), 76-0079 (20 μM), Orlistat (20 μM), and PMSF (1 mM). Additionally, cell

lysates were heat inactivated at 60 °C for 10 min. Data are shown as mean + S.D. and representative for three independent experiments ($n = 3$). Statistically significant differences were determined by Student's unpaired *t*-test (two-tailed; *, $p < 0.05$; **, $p < 0.01$; ***, $p < 0.001$).

Europe PMC Funders Author Manuscripts

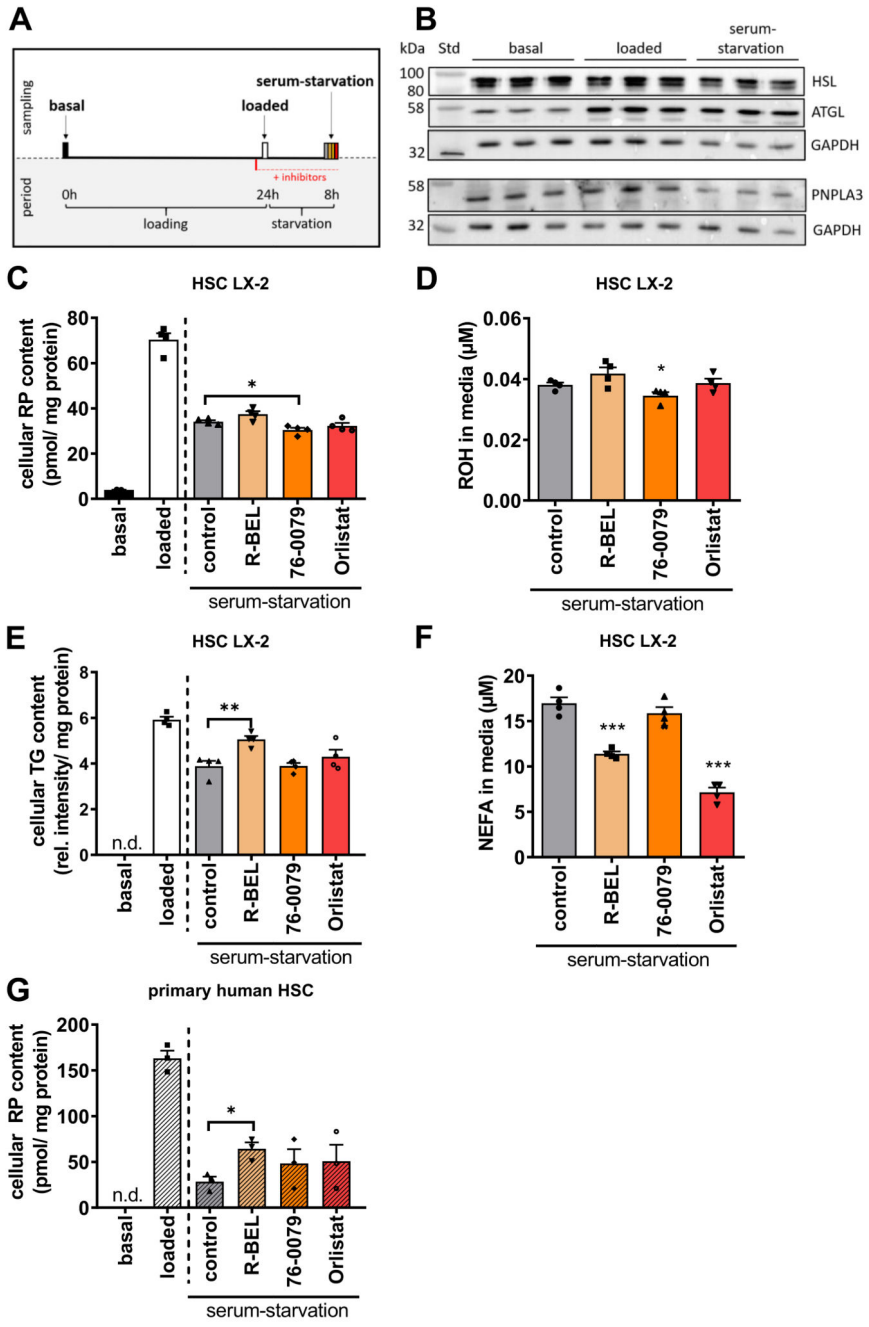

Fig. 2. ATGL, PNPLA3, and HSL are not limiting for the breakdown of REs in human HSCs.

(A) Schematic presentation of pulse-chase experiment. (B–G) LX-2 or primary human HSCs were plated in 12-well or 24-well plates and cultured in DMEM containing 1% or 10% FCS for 24 h, respectively (= basal). Then, cells were incubated with DMEM containing 10% FCS, ROH (40 µM or 20 µM), and oleic acid (300 µM or 100 µM) for 24 h (= loaded). Media were changed to DMEM low glucose (1 g/l) containing 2% FA-free BSA for 8 h (= serum-starvation). Serum-starvation media contained small molecule inhibitors or solvent as indicated: DMSO (solvent control), R-BEL (20 µM), 76-0079 (20 µM), or Orlistat (20 µM).

Europe PMC Funders Author Manuscripts

(B) Protein expression levels of HSL, ATGL, and PNPLA3 in LX-2 cell lysates were determined by Western blot analyses using specific antibodies. Anti-GAPDH antibody was used as loading control. (C, E, G) Cellular lipids were extracted with *n*-hexane:2-propanol (3:2, v/v). (C, G) RP and (E) TG contents were determined by HPLC-FD and thin-layer chromatography, respectively. Band intensities corresponding to TG were quantitated by Bio-Rad Image Lab Software. (D) Serum-starvation media were *n*-hexane extracted and ROH content determined by HPLC-FD. (F) NEFA content of serum-starvation media was determined by commercial NEFA kit (Wako Chemicals). Cellular lipid contents were normalized to cell protein. Data are shown as mean + S.D. and representative for two to four independent experiments ($n = 3–4$). Statistically significant differences were compared to DMSO control and determined by Student's unpaired *t*-test (two-tailed; *, $p < 0.05$; **, $p < 0.01$; ***, $p < 0.001$). *n.d.* = not detectable.

Europe PMC Funders Author Manuscripts

Europe PMC Funders Author Manuscripts

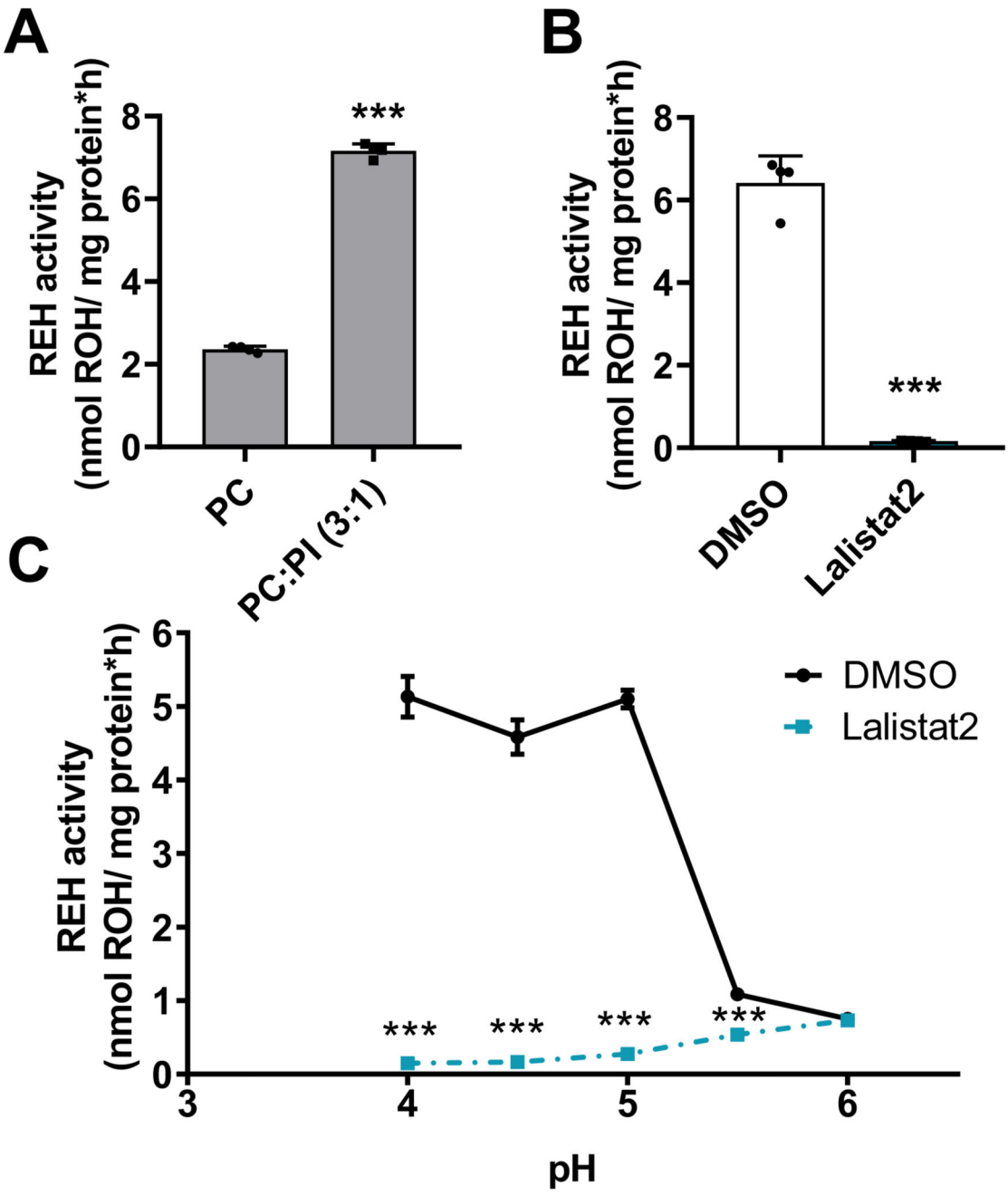

Fig. 3. LAL accounts for the majority of acid RE hydrolase activity in human HSC cell-line LX-2.

(A) Cell lysates of LX-2 cells (1000 × *g* supernatant) were incubated with RP (150 μM) as substrate for 1 h. Substrates were emulsified with PC (150 μM) or PC:PI (3:1, M/M, 150 μM) in potassium acetate buffer (50 mM, pH 4.5). (B) Cell lysates of LX-2 cells were incubated with RP and emulsified with PC:PI (3:1, M/M, 150 μM) as described in A. The incubation mixture contained either DMSO (solvent control) or Lalistat2 (20 μM). (C) Cell lysates of LX-2 cells, containing DMSO or Lalistat2, were incubated with RP emulsified with PC:PI (3:1, M/M) in potassium chloride buffer (50 mM). pH of incubation mixtures

was adjusted by addition of potassium acetate buffer of indicated pH. (A–C) Lipids were *n*-hexane extracted and ROH content was determined by HPLC-FD. Data are mean + S.D. and representative for two independent experiments ($n = 4$). Statistically significant differences were determined by Student's unpaired *t*-test (two-tailed; ***, $p < 0.001$).

Europe PMC Funders Author Manuscripts

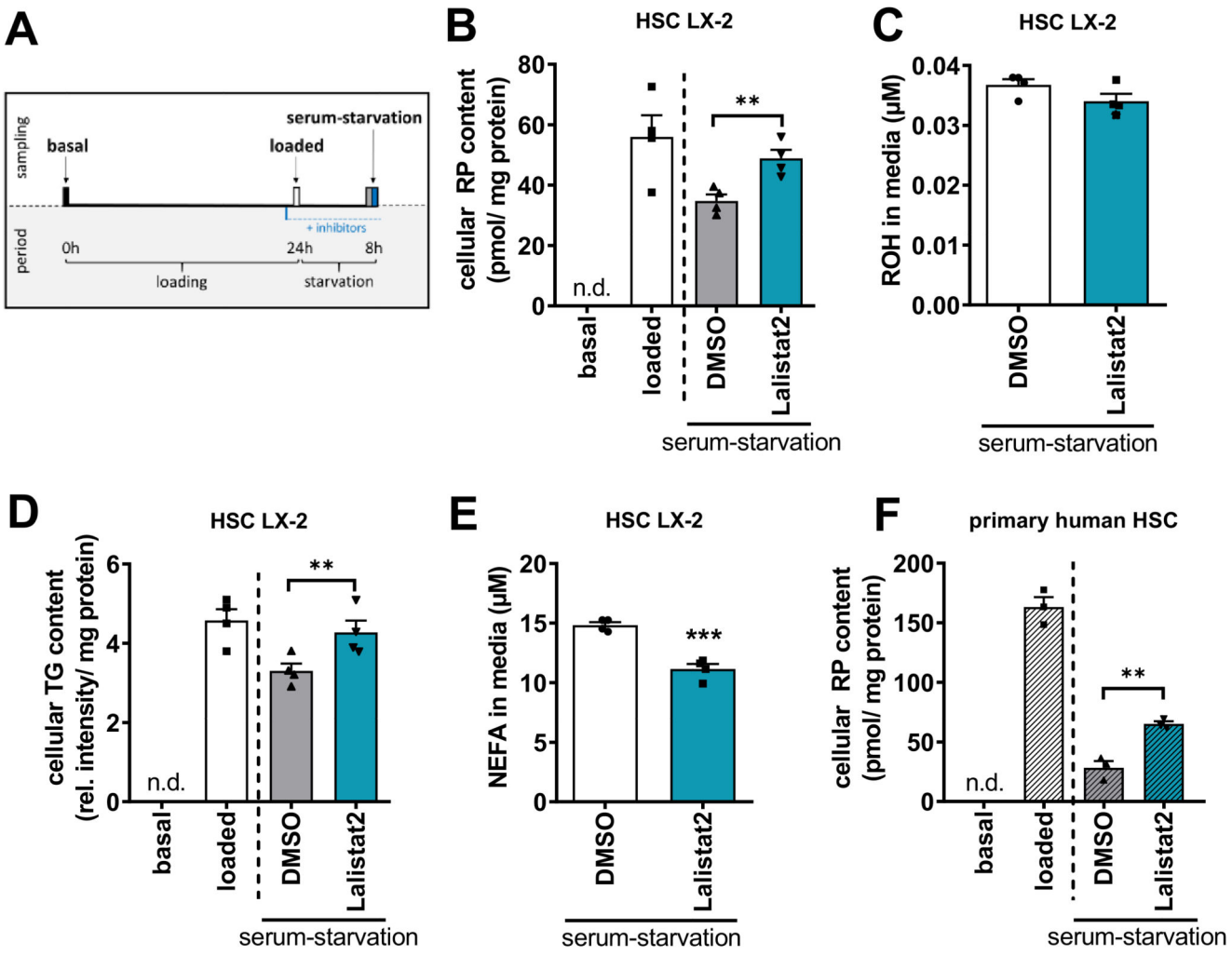

Fig. 4. LAL-specific inhibitor Lalistat2 partially inhibits the breakdown of REs of human HSCs.

(A) Schematic presentation of pulse-chase experiment. (BeF) LX-2 or primary human HSCs were plated in 12-well or 24-well plates and cultivated in DMEM containing 1% or 10% FCS, respectively (= basal). The next day, cells were incubated with DMEM containing 10% FCS, ROH (40 µM or 20 µM), and oleic acid (300 µM or 100 µM) for 24 h (= loaded). Subsequently, cells were incubated with DMEM (1 g glucose/l) containing 2% FA-free BSA for 8 h (= serum-starvation). Serum-starvation media contained DMSO (solvent control) or Lalistat2 (20 µM). (B, D, F) Cellular lipids were extracted with *n*-hexane:2-propanol (3:2, v/v). (B, F) RP and (D) TG contents were determined by HPLC-FD and thin-layer chromatography, respectively. Band intensities corresponding to TG were quantitated by Bio-Rad Image Lab Software. (C) Serum-starvation media were *n*-hexane extracted and ROH content was determined by HPLC-FD. (E) NEFA content of serum-starvation media was determined by commercial NEFA kit. Cellular lipid contents were normalized to cell protein. Data are shown as mean + S.D. and representative for two to four independent experiments (n = 3–4). Statistically significant differences were compared to DMSO control

and determined by Student's unpaired *t*-test (two-tailed; **, $p < 0.01$; ***, $p < 0.001$). *n.d.* = not detectable.

Europe PMC Funders Author Manuscripts

Europe PMC Funders Author Manuscripts

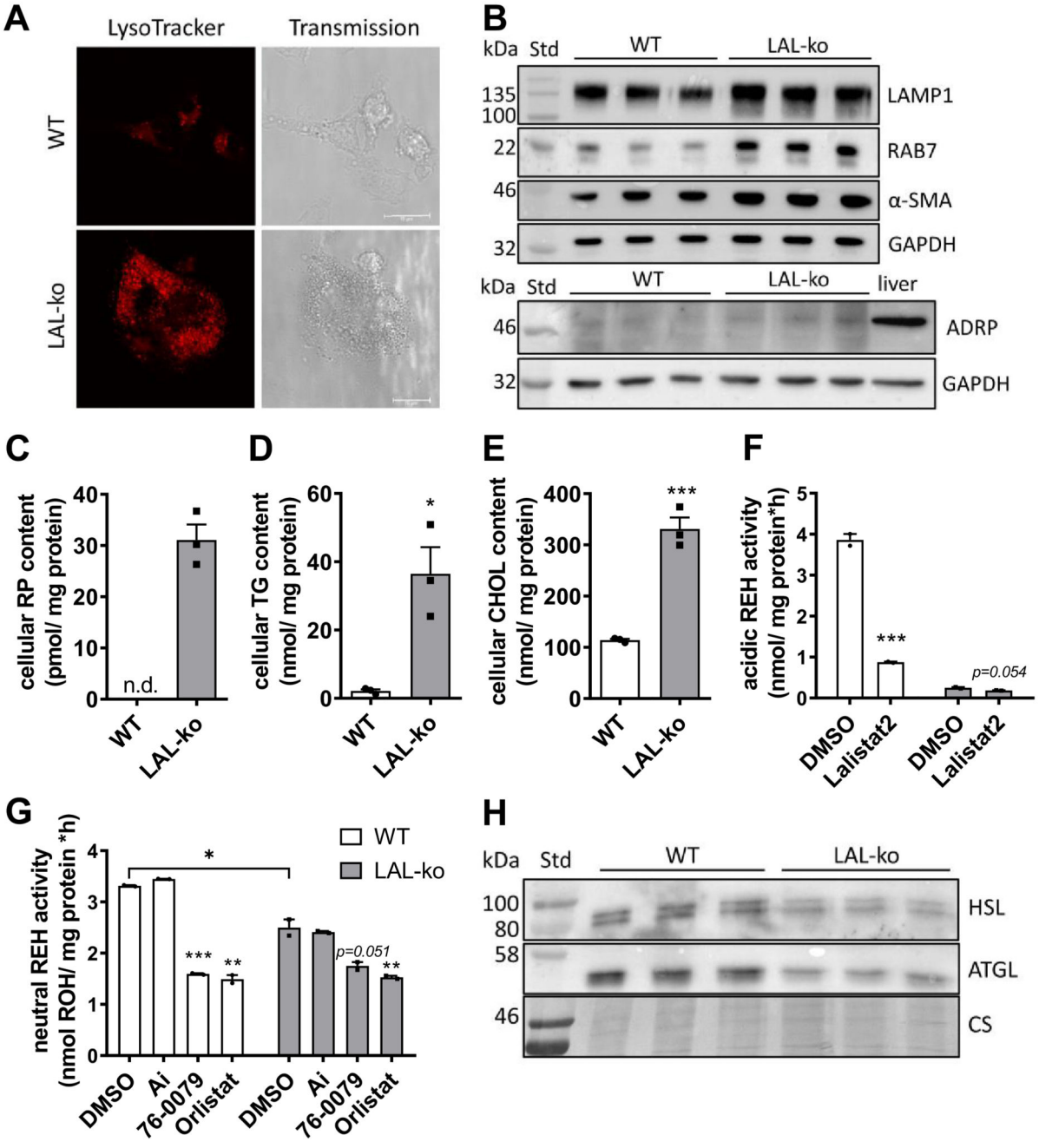

Fig. 5. Primary HSCs from LAL-deficient mice exhibit accumulation of lysosomes and REs.

Primary HSCs from WT and LAL-ko mice were isolated by collagenase digestion and cultivation for 14 days in ROH (5 μM) containing media. (A) Primary WT and LAL-ko HSCs were incubated with LysoTracker Red DND-99 for 45 min. Fluorescence of the LysoTracker dye was recorded by laser-scanning live cell imaging. Transmission images visualize cell structures. (B) Protein expression of lysosomal markers LAMP1 and RAB7, HSC activation marker α-SMA, and lipid droplet marker ADRP was determined by Western blotting. Liver lysate (1000 × g supernatant, of fasted mice) was used as control. (C-E)

Neutral lipids of primary HSCs from WT and LAL-ko mice were extracted with *n*-hexane:2-propanol (3:2, v/v). Dried lipids were dissolved (C) in methanol:toluene (1:1, v/v) and RP levels were determined by HPLC-FD analysis, or (D, E) in 0.1% Triton X-100 and TG and total CHOL content were determined by commercial triglyceride™ infinity (Thermo Fisher Scientific) and CHOD-PAP kit (Roche Applied Science), respectively. (F, G) Cell lysates (1000 × g supernatant) of WT and LAL-ko primary HSCs were incubated with RP (150 μM) as substrate for 1 h. (F) Substrate was emulsified with PC:PI (3:1, M/M, 150 μM) in sodium acetate buffer (100 mM, pH 4.5). The incubation mixture contained Lalistat2 (10 μM) or DMSO (solvent control). (G) Substrate was emulsified with PC (150 μM) in potassium phosphate buffer (100 mM, pH 7.5). The incubation mixture contained Ai (10 μM), 76-0079 (10 μM), Orlistat (10 μM), or DMSO (solvent control). Lipids were *n*-hexane extracted and ROH content was determined by HPLC-FD. (H) Protein expression of HSL and ATGL was determined by Western blotting using specific antibodies. Coomassie stain (CS) was used as loading control. Data are mean + S.D. and are representative for three independent experiments ($n = 3$). Statistically significant differences were compared to WT HSCs and determined by Student's unpaired *t*-test (two-tailed; *, $p < 0.05$; **, $p < 0.01$; ***, $p < 0.001$). n.d. = not detectable.

Europe PMC Funders Author Manuscripts

Europe PMC Funders Author Manuscripts

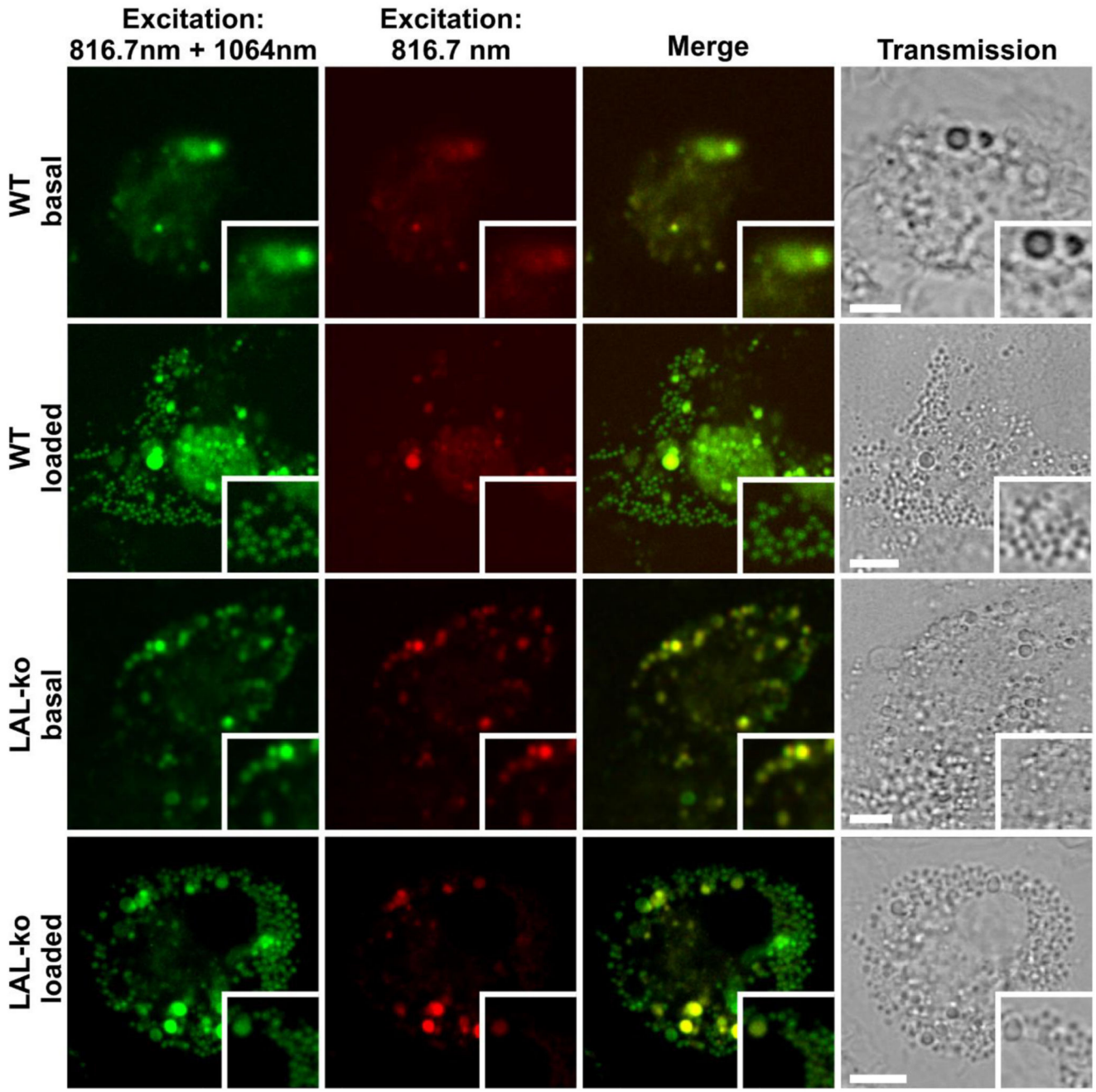

Fig. 6. Neutral lipid stores of primary murine WT and LAL-ko HSCs are increased upon lipid loading.

Primary murine WT and LAL-deficient HSCs (= LAL-ko) were isolated by selective detachment for 14 days in DMEM containing 10% FCS and ROH (5 μM). Cells were plated in 8-well chamber slides. The next day, media were changed to DMEM containing 10% FCS (= basal) or DMEM containing 10% FCS, ROH (20 μM), and oleic acid (100 μM) (= loaded). Cells were further incubated overnight. Images of CARS signal (Ex. 816.7 nm + 1064 nm) and autofluorescence (Ex. 816.7 nm) were recorded and merged. Insets depict

selected areas of the images. Transmissions images visualize cell structures. Scale bar = 5 μm.

Europe PMC Funders Author Manuscripts

Europe PMC Funders Author Manuscripts

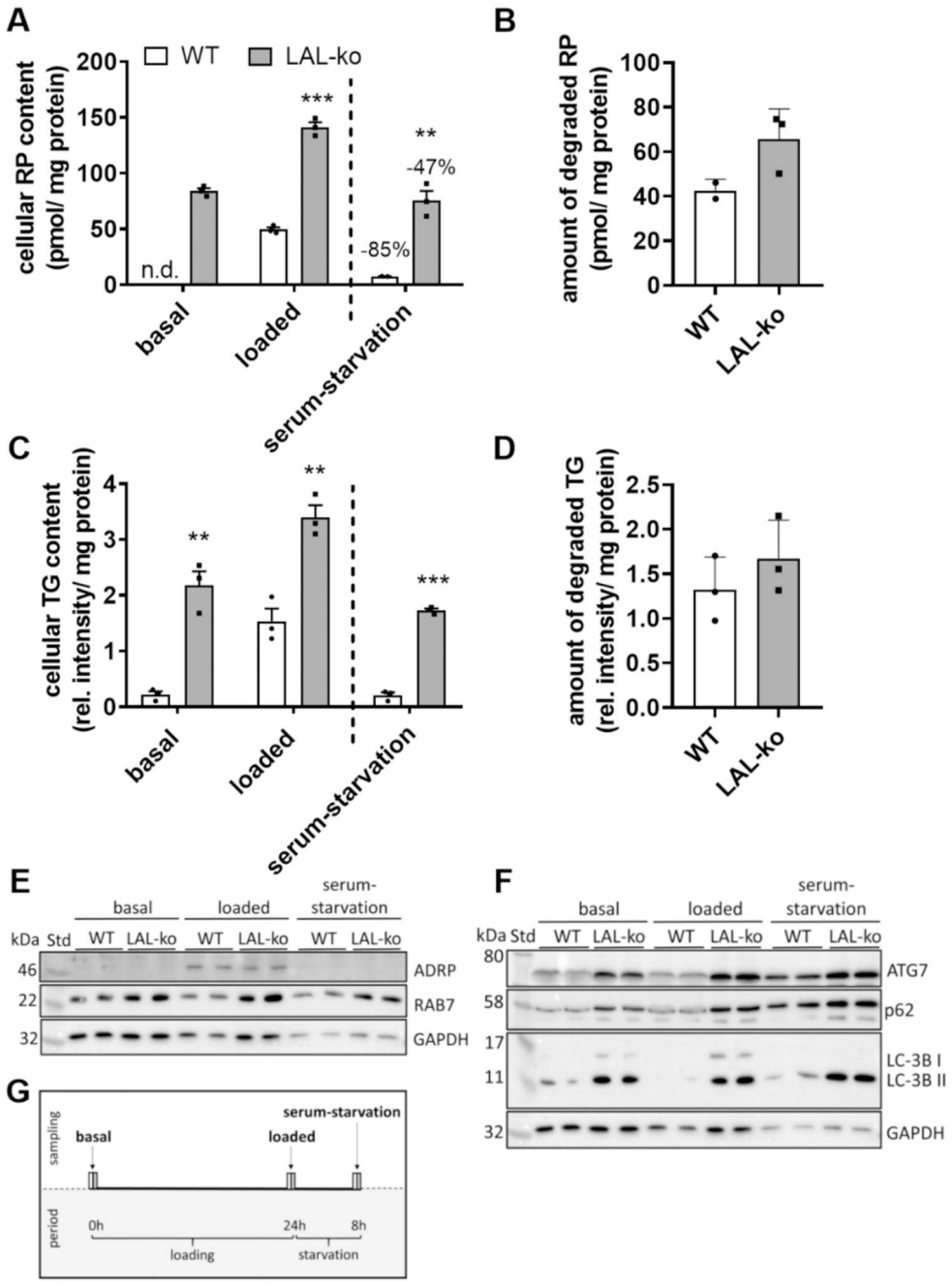

Fig. 7. LAL-deficient murine HSCs lose RE stores under serum-starvation.

Primary HSCs were isolated from WT and LAL-ko mice by collagenase digestion and cultivation for 14 days in DMEM media containing 10% FCS and ROH (5 μM). (A–F) HSCs were plated in 6-well plates and cultivated in DMEM containing 10% FCS (= basal). The next day, cells were incubated with DMEM, containing 10% FCS, ROH (20 μM), and oleic acid (100 μM) for 24 h (loading period). Media were changed to DMEM low glucose (1 g/l) supplemented with 2% FA-free BSA for 8 h (serum-starvation period). (A) Lipids were extracted with *n*-hexane:2-propanol (3:2, v/v) and RP content was determined by

HPLC-FD. (C) Lipid extracts were separated by thin-layer chromatography. Band intensities corresponding to TG were quantitated by Bio-Rad Image Lab Software and normalized to mg cell protein. (B, D) Amount of degraded RP and TG were calculated by subtracting the amounts after “serum-starvation” from that of “loaded” cells. (E, F) Protein expressions of the lipid droplet marker ADRP (E) and autophagy markers ATG7, p62, and LC-3 I and II (F) were analyzed by Western blot analyses. (H) Schematic presentation of pulse-chase experiment. Data are mean + S.D. and representative for three independent experiments (n = 3). Statistically significant differences were determined by Student's unpaired t-test (two-tailed; **, $p < 0.01$; ***, $p < 0.001$). *n.d.* = not detectable.

Europe PMC Funders Author Manuscripts